



Tânia Santos Lopes

Bachelor in Micro and Nanotechnologies Engineering

Simulation and development of paper-based actuators

Dissertation submitted in partial fulfillment

of the requirements for the degree of

Master of Science in

Micro and Nanotechnologies Engineering

Adviser: Dr. Diana Gaspar, Senior Researcher, AlmaScience

Co-adviser: Prof. Luís Miguel Nunes Pereira, Associate Professor, DCM, FCT-UNL

Examination Committee

President: Prof. Dr. Rodrigo Martins

Examiner: Prof. Dr. Joana Sarmento

Supervisor: Dr. Diana Gaspar

Junho de 2021

Simulation and development of paper-based actuators

Copyright © Tânia Santos Lopes, Faculdade de Ciências e Tecnologia,

Universidade Nova de Lisboa, 2020.

A Faculdade de Ciências e Tecnologia e a Universidade Nova de Lisboa têm o direito, perpétuo e sem limites geográficos, de arquivar e publicar esta dissertação através de exemplares impressos reproduzidos em papel ou de forma digital, ou por qualquer outro meio conhecido ou que venha a ser inventado, e de a divulgar através de repositórios científicos e de admitir a sua cópia e distribuição com objetivos educacionais ou de investigação, não comerciais, desde que seja dado crédito ao autor e editor.

Acknowledgements

Firstly, I would like to thank Prof. Dr. Elvira Fortunato and Prof. Dr. Rodrigo Martins for the creation and divulgation of this new Engineering course. A special thank you also, for the opportunity of making my master thesis in those highly regarded facilities that are CENIMAT|i3N and CEMOP, where the investigation conditions are exceptional.

Secondly, I would like to give a special thank you to my Advisor, Dr. Diana Gaspar, for all the support and for always being available, for her advice and knowledge transmission.

To my Co-advisor, Prof. Dr. Luís Pereira for the opportunity to join this project and your team. To Prof. Aaron Mazzeo who introduced me to this thesis theme and whom I had the pleasure to meet.

To all the group at paper laboratory and the team at CENIMAT|i3N that helped during this period whenever I needed.

To all the friends I made throughout this course, specially Kika, Inês and Diogo. My godmother and my goddaughter. The futsal, for always being there for me and for all the joyfull moments.

Finally, I would like to thank my family, without whom this journey would be impossible. Without them I would not be the person I am today and without their support this experience would have never happened.

Thank you all.

Abstract

Soft robots have become an attractive research topic for opening new doors for robots' limitations by being flexible, light, and small and with the ability to have an adaptable shape. An essential component in a soft robot is the soft actuator, which provides the system with a deformable body and allows it to interact with the environment to achieve the desired actuation pattern. Among the various materials used in soft actuators, paper-based actuators have special attention because paper is an abundant, lightweight, and biodegradable material.

This work illustrates an insight into the soft actuators field and focuses on developing unique paper-based actuators applying the microwave heat for a liquid-vapor phase transition, in this case, water. This document focuses on the study of different designs, materials, and thicknesses by changing the paper, elastomer, and double-sided tape.

Keywords: Soft actuators; paper; microwave heat; liquid-vapor phase transition

Resumo

Os robôs flexíveis tornaram-se um tópico de pesquisa atraente por abrirem novas portas para as limitações dos robôs por serem flexíveis, leves e pequenos e com a capacidade de ter uma forma adaptável. Um componente essencial em um robô flexível é o atuador flexível, que fornece ao sistema um corpo deformável e permite que este interaja com o ambiente para atingir o movimento desejado. Dos vários materiais usados em atuadores flexíveis, os atuadores baseados em papel têm especial atenção porque o papel é um material abundante, leve e biodegradável.

Este trabalho ilustra uma visão da área de atuadores flexíveis e foca no desenvolvimento de atuadores únicos baseados em papel, aplicando o calor de microondas para uma transição de fase líquido-vapor, neste caso, água. Este documento mostra o estudo de diferentes designs, materiais e espessuras, alterando o papel, elastômero e fita dupla-face.

Palavras-chave: Atuadores flexíveis; papel; aquecimento por microondas; transição de fase líquido-vapor

Contents

Acknowledgements	iii
Abstract	iv
Resumo.....	v
Contents.....	vi
List of Figures	vii
List of Tables.....	ix
Acronyms	x
Objectives and Motivation	xi
1 Introduction.....	1
1.1 Soft robots actuators.....	1
1.1.1 Photo-responsive actuators	2
1.1.2 Magnetically responsive actuators.....	4
1.1.3 Electrically responsive actuators	5
1.1.4 Pressure-driven actuators.....	6
1.1.5 Thermally responsive actuators.....	8
1.2 Pneumatic actuation	11
1.3 Soft materials for soft actuators.....	12
1.3.1 Cellulose actuators.....	14
2 Materials and Methods.....	17
2.1 PDMS, PMMA and Ecoflex 30 solutions	17
2.2 Doctor Blade.....	17
2.3 UV	17
2.4 Laser cutting of layers	17
2.5 Metallic nanoparticles	18
2.6 Thermal analysis.....	18
3 Results and Discussion.....	19
3.1 Simulation of the actuator	19
3.2 Production of the simulated actuator	21
3.3 Paper-based actuators	23
3.4 Thermal analysis.....	28
4 Conclusion and Future perspectives.....	34
References.....	35
Annex	38

List of Figures

- Figure 1.1 - Different classes of soft actuators based on the stimulation type (from [4]). 2
- Figure 1.2 - The shape memory effect in the liquid crystal polymer film (a) before dual light treatment (b) subjected to dual light illumination and deformed into a curled shape (c) shape after the dual light treatment (d) recovered initial shape by dual light exposure [7]. 3
- Figure 1.3 - Photograph of photochromic superabsorbent polymers (a) dry and (b) swelled with water [9]. 3
- Figure 1.4 - Schematic showing the fabrication sequence: a) Loading the cellulose matrix with ferrofluid and b) laser micromachining [11]. 4
- Figure 1.5 - Snapshots of a soft-tissue-paper ferropaper actuator ($0.8 \text{ mm} \times 8 \text{ mm} \times 25 \text{ }\mu\text{m}$) excited by a 46 mT sinusoidal (10 Hz) magnetic field [11]. 5
- Figure 1.6 - Dielectric elastomer operating principle. When a bias voltage is applied across an elastomer film coated on both sides with compliant electrodes, Coulombic forces act to compress the film in the thickness direction and expand it in plane [14]. 5
- Figure 1.7 - Working principle of the phase change actuator. (a) A cavity within an elastomer is filled with a low-boiling point liquid. Heating of the liquid above its boiling point is achieved with a SMD resistor within the liquid connected to a battery. The cavity is sealed with an elastomer membrane. (b) Upon resistive heating the liquid evaporates and the thin membrane strongly deforms into a balloon shape [17]. 6
- Figure 1.8 - Basic configurations and sequential actuation of subgroups of embedded bladders for two types of rotary actuators. a) Subgroups of bladders inflating around fixed stators in peristaltic fashion ($1 \rightarrow 2 \rightarrow 3 \rightarrow 4 \rightarrow 1 \dots$). Four different colors mark the four subgroups, respectively. b) An actuator with an internal rotor (Type 1) showing a step angle of 22.5° , along with rotation between stable states (enclosed by the dashed lines). c) An actuator with an external rotor (Type 2) showing a step angle of 22.5° and rotation between stable states (enclosed by the dashed lines) [19]. 7
- Figure 1.9 – 1) Basic principle of an all PDMS bending PBA consisting of two PDMS films with different thicknesses or material properties: (a) schematics; (b) photographs. 2) A schematic view of the microfingers composed of two opposing PBAs. Normally, closed microfingers that are open due to the bending motion of the PBAs [20]. 8
- Figure 1.10 - Unique combined features of PNIPAm and PPy provide innovative multiple functions. Thermo-responsive volumetric change induces deformable bending or variation in electrical conductivity. Membranes of various shapes can be fabricated by utilizing photopolymerization patterning. Variation in membrane surface charge can be used for selective filtration of charged molecules [24]. 9
- Figure 1.11 - A wireless ultrathin bellows-style actuator before and during actuation. The thicker connection is kept to ease filling by a syringe and is not an essential part of the actuator. a) Before actuation. b) During actuation [36]. 11
- Figure 1.12 - a) Schematic representation of the fabrication of the HEPAs: i) wax is printed and melted into the paper to form the fluidic channels; ii) a suspension of PEDOT:PSS is added to the channels; iii) the water evaporates and deposits the conducting film of PEDOT:PSS

in the channel; iv) a piece of tape is attached to the paper/PEDOT:PSS composite to act as a strain-limiting layer. b) Photograph of the wax patterned channel. c) Photograph of the paper/PEDOT:PSS composite. d) Photograph of the cross-section showing that the PEDOT:PSS is embedded in the paper channel. e) Schematic representation of the four HEPAs (straight, precurved, creased-curved, and creased-sawtooth) and their motion of actuation; L, length; W, width [45]. 15

Figure 3.1 - First design of simulation, an actuator using PDMS and acrylic as materials and having a maximum displacement of 1 mm in the red area, obtained with pressure. 19

Figure 3.2 - Another design of an actuator assembled with a) the PMMA layer, b) the PDMS layer and c) the layer of Ecoflex 30..... 20

Figure 3.3 - The simulation of the actuator with the layout in the picture above, using Ecoflex 30 on the bottom, PDMS and PMMA on top. a) a pressure of about 0.6 kPa was applied leading to a displacement of about 1.3 mm, while when b) a pressure of 1 kPa is reached in the joint with PDMS to form a bladder with a maximum stretch of near 3 mm..... 20

Figure 3.4 - Four actuators put together, operating at the same time, to form a small robot, using pressure to obtain a maximum stretch of 1.3 mm..... 21

Figure 3.5 - Structure of the actuators made according to the structure used in the simulation made with Ecoflex 30 (40x20 mm), PMMA (19 x 20 mm) and PDMS (6 x 20 mm). 21

Figure 3.6 – Some examples of the actuators made with Ecoflex 30, PMMA and PDMS with different thicknesses. 22

Figure 3.7 – Experiment of the adhesion between PDMS and Ecoflex 30 after UV treatment: 1) both PDMS and Ecoflex 30 with UV; 2) only Ecoflex 30 with UV; 3) only PDMS with UV; 4) PDMS and Ecoflex 30 with UV and PMMA between them without treatment. 22

Figure 3.8 – Assembly of the first actuators made according to the structure used in the simulation made with latex, paper soaked in water and tape on top. 24

Figure 3.9 - Actuator tested during 1 minute in the microwave oven at 800 W. 24

Figure 3.10 – Structure of the second actuator, using latex, double-sided tape, paper with water and acetate with superficial cuts in the middle to be more flexible..... 24

Figure 3.11 – Different areas of the inflated zones. a) 1.44 cm²; b) and c) 2.28 cm²; d) 3 cm²; e) 3.61 cm² and f) 4.75 cm². 27

Figure 3.12 – Thermal image of the actuator that had the most significant motion..... 28

Figure 3.13 – a) The solution of the metallic nanoparticles: copper 40 nm; zinc 10 μm and zinc <150 μm; b) paper with gold nanoparticles and c) silver nanowires with fibrillated cellulose fibers..... 28

Figure 3.14 – Structure similar as in Figure 3.10: a) with a solution of metallic nanoparticles; b) paper with Au/Ag nanoparticles with adjacent wet paper. 29

List of Tables

Table 1.1 - Advantages and limitations of various actuation types.....	10
Table 1.2 - Materials used for different external stimuli [3], [4].	13
Table 1.3 - Paper-based Thermal Actuation.....	16
Table 2.1 - Different power and speed used for which material.	18
Table 3.1 - Indication of Young's Modulus for which material, according to the literature [61]– [64].	23
Table 3.2 – Experiment of different volumes of water in the actuators.	25
Table 3.3 - Results of testing acetate, cellophane, Kapton, properties of porous paper and different kinds.	26
Table 3.4 – Results testing between Whatman paper n°1 (181 μm) and whatman paper (80 μm).	27
Table 3.5 - Results by thermal camera and movement of actuators made with zinc (10 μm) for different concentrations and times.....	30
Table 3.6 - Results by thermal camera and movement of actuators made with copper 40 nm for different concentrations and times.....	31
Table 3.7 - Results by thermal camera and movement of actuators made with zinc <150 μm , gold nanoparticles and silver nanowires for different times.....	32
Table 3.8 – Summary of actuator temperatures by thermal analysis with and without metallic nanoparticles for different times.....	33
Table A.1 - Results of testing different elastomers and double-sided tapes.	38

Acronyms

CNT - Carbon nanotube
DE - Dielectric elastomer
DEAP - Dielectric electroactive polymer
EAP - Electroactive polymer
EAPap - Cellulose-based electroactive paper
EC - Ethylene carbonate
ECF - Electroconjugate fluid
ERF - Electrorheological fluid
HEPA - Hygroexpansive Electrothermal Paper Actuator
HM - Hybrid membrane
IPMC - Ionic-polymer-metal composite
IR - Infrared radiation
LCE - Liquid-crystal elastomer
LCP - Liquid-crystal polymer
LCN - Liquid-crystal polymer network
LCST - Low critical solution temperature
MEMS - Microelectromechanical system
MRF - Magnetorheological fluid
NIR - Near-infrared radiation
NP - Nanoparticle
NW - Nanowire
PBA - Pneumatic balloon actuator
PDMS - Polydimethylsiloxane
PMMA - Polymethylmethacrylate
PNIPAm - Poly(N-isopropylacrylamide)
PPI - Pulses per inch
PPy - Poly(pyrrole)
PVA - Polyvinyl alcohol
RGB - Color code referring to red, green and blue
SMP - Shape memory polymer
THF - Tetrahydrofuran
ULS - Universal Laser System
UV – Ultraviolet light

Objectives and Motivation

The main goal of this master thesis is to show a review of the field of soft actuators and the soft materials normally used. Those materials which can be easily compressed, cut, bent or scratched are called soft materials. In this thesis it is showed a component more theoretical. It is also presented some experimental results based on simulating and development of paper-based actuators in a way never made before, using steam as a working fluid heated with microwaves to inflate bending joints/bladders. Therefore, different materials are used in order to achieve greater motion in the actuator and also to make it cheap, weightless, and very thin. This dissertation is concerned with the development of paper-based actuators that can:

- Trigger motion with steam
- Work without the use of external components
- Simple to produce

1 Introduction

Over the years, robots have been substituting man's work in the most diverse areas. Robots first appeared as robust metal structures (hard robots) and were a great help in developing technology. However, robot became more than a tool for industrial manufacturing, being nowadays considering for human-machine interactions and as consequence, a new field of robotics appeared: soft robotics.

1.1 Soft robots actuators

Soft robots emerged to overtake service robots' limitations, such as, low-cost user-oriented operation systems, but mainly in terms of implications for human-machine interactions. In natural environments, the observation of the role of compliance in animals and plants allows soft robots to explore some underlying mechanical properties, such as elasticity, viscosity, softness, density, and stickiness. They have an essential role in robotics innovation because they can achieve complex motion, have an adaptable shape, and be compatible with human interaction while being mechanically resilient and enabling low-cost manufacturing. Soft robots can also be used for sensory devices and actuators [1], [2].

In specific, soft robots present additional challenges because their sensing and actuation devices are generally highly integrated within the robot body and its whole functionality. These challenges become even more critical when the soft robot is scaled down to micro-size as they often lack on-board power, sensing, computation, and control. As a result, soft actuators have been miniaturized to respond to various stimuli and show large deformations in addition to mechanical resilience that is crucial. These would be particularly promising for applications in artificial muscles, microrobots, micro-manipulators, cell scaffolds, micro lenses, and smart transforming sheets while adding diverse multifunctionality, including drug delivery, sensing, biodegradability and biocompatibility, and color change. An essential component in a soft robot is the soft actuator, which provides the system with a deformable body and allows it to interact with the environment to achieve the desired actuation pattern [3], [4].

Soft actuators typically convert various forms of input energy into output energy. As shown in Figure 1.1 - Different classes of soft actuators based on the stimulation type (from [4]). the input energy might be in the form of light, heat, applied electric and magnetic fields, or with pressure, while the output energy is usually mechanical. These devices execute a physical motion or induce a force in response to a controlled input signal, which changes its environment. Regarding movement, actuators might provide the linear, rotary, and bending motions, which depend on the design of the device. Soft actuators are not only flexible but also demonstrate high power to density ratio, low weight, less pollution, and noise-free operation. Soft actuators can even realize complex and multiple degrees of freedom outputs motions with simple control inputs [4], [5].

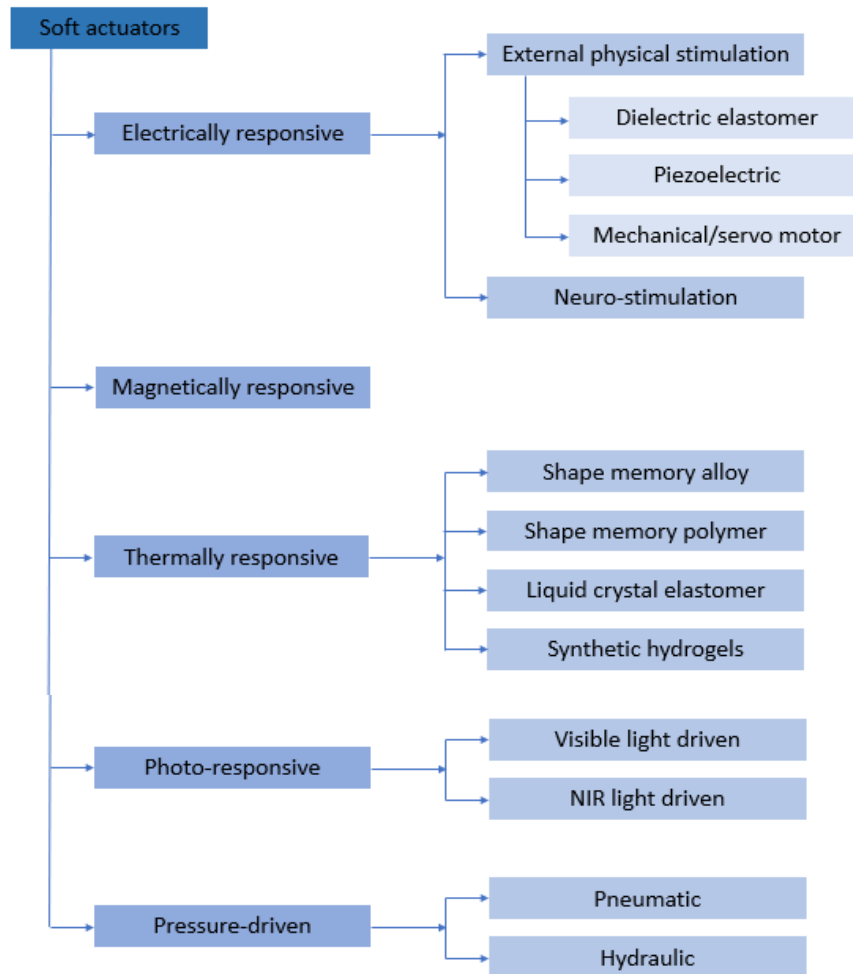


Figure 1.1 - Different classes of soft actuators based on the stimulation type (from [4]).

1.1.1 Photo-responsive actuators

Photo-responsive actuators have been extensively explored in designing various devices and structures, showing the capability to convert optical signals that can be visible light or near-infrared (NIR), into mechanical work. Light-induced soft actuation is compelling because it can be remotely and accurately controlled, rapidly modulated, and easily focused on nano and microscale areas. Photo-responsive materials are based on photochromic molecules, which capture optical signals and convert them into different property modifications. Photochromic molecules play a major role in synthetic photo-responsive systems, capturing optical signals and translating these to useful property changes such as strain. These molecules can be integrated into various soft actuators, including gels, polymers, fluid, and photostrictive materials [3], [6].

In 2016, Kumar *et al.* reported the fabrication of a shape memory polymer liquid crystal network film that switches between two geometrical shapes using light rather than temperature. In their work, they modulated a crosslinked liquid crystal network's mechanical properties by

exposing it to light. They found that when adding a small amount of copolymerized azobenzene crosslinker, it reduced the elastic modulus when addressed with ultraviolet (UV) light (365 nm) and blue light (455 nm). Also, with an optimized crosslinker content, they were capable of switching the polymer from its glassy state to its rubber state. Figure 1.2 illustrates the light-induced shape memory of low crosslinked liquid crystal network [7].

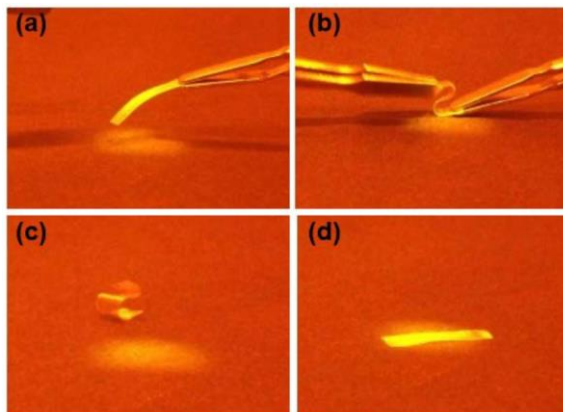


Figure 1.2 - The shape memory effect in the liquid crystal polymer film (a) before dual light treatment (b) subjected to dual light illumination and deformed into a curled shape (c) shape after the dual light treatment (d) recovered initial shape by dual light exposure [7].

Regarding the application of photoreactive gels as actuators, Sakai *et al.* demonstrated that by adding azobenzene chromophores as crosslinkers they obtained a gel expansion of 80-100 % under UV light and contraction under visible light [8]. It was similarly reported by K. Thilini *et al.*. They prepared superabsorbent hydrogels stimulated by azobenzenes enabling the gel to liquefy under UV light [9]. Figure 1.3 shows the photographs taken on the dry and swollen photochromic superabsorbent polymers.

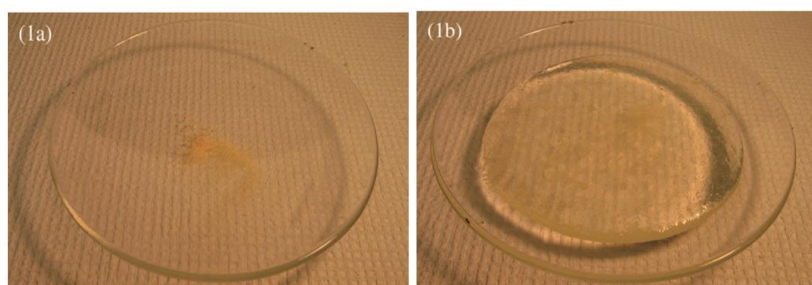


Figure 1.3 - Photograph of photochromic superabsorbent polymers (a) dry and (b) swelled with water [9].

“Light-Driven Motion of Liquids on a Photoresponsive Surface” by Ichimura *et al.* records the manipulation of the motion of an olive oil droplet on a flat solid surface by photoirradiation (asymmetrical UV and blue light irradiation) of an azobenzene monolayer covering the surface. Azobenzenes are isomerized by shining light on the surface, producing a gradient of free surface energy. Firstly, the droplet undergoes a reduction in diameter, raising the touch angles on both

the forward and receding edges. Gradually, the droplet continues to travel at speeds of $35 \mu\text{m s}^{-1}$. The direction and velocity of the motion were adjusted by altering the light intensity. The light-driven motion of a fluid substance in a surface-modified glass tube suggests potential applicability to microscale chemical process systems [10].

1.1.2 Magnetically responsive actuators

Magnetic stimulation is considered interesting especially because it can quickly and precisely control the magnetic field direction and magnitude, in addition to its ability to penetrate most materials. This is promising for applications restricted to enclosed areas such as targeted drug delivery, microfluidics, microsurgery, and assembly within the body.

Soft composites, such as polymers, gels, papers, and fluids, with magnetic fillers, can be actuated with an external magnetic field. The insertion of discrete magnetic fillers into soft compounds results in a magnetization profile with variable magnitude and direction. When a magnetic field is applied to these actuators, the embedded magnetic particles or the attached permanent magnets try to align with the field, generating deformation, torques, bending, elongation, and contraction. These actuation modes are generally generated when the spatial field gradients interact with the magnetic fillers. However, in small areas, both the field and its spatial gradients can be created independently, allowing for two independent actuation modes needed for complex motions [3], [4].

Ding *et al.* fabricated miniature magnetic actuators using ferrofluid-impregnated paper and did testing in different papers such as soft tissue paper, cleanroom paper, Whatman n°1 filter paper, printer paper, and newspaper. For the assembly of these devices, a ferrofluid based on light mineral oil was placed on each paper. After the ferropaper was dried in the oven, the paper was cut with a laser creating a cantilever pattern, as Figure 1.4 shows [11].

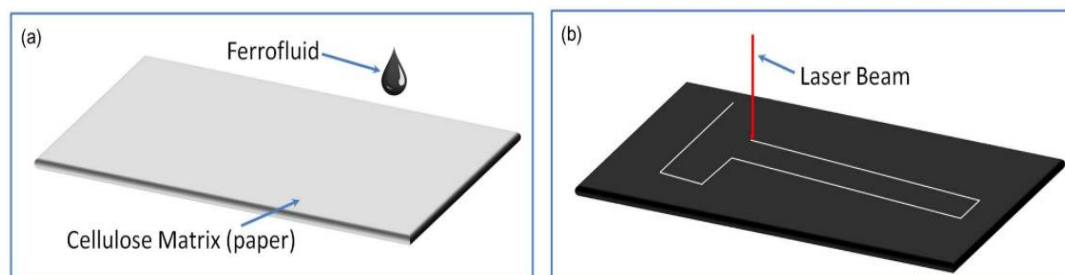


Figure 1.4 - Schematic showing the fabrication sequence: a) Loading the cellulose matrix with ferrofluid and b) laser micromachining [11].

After the tests with the different papers, Ding *et al.* demonstrated that the soft-tissue-paper cantilever had the largest bending angle (58°) under ac excitation (10 Hz) with a magnetic field amplitude of 46 mT, as Figure 1.5 illustrates [11].

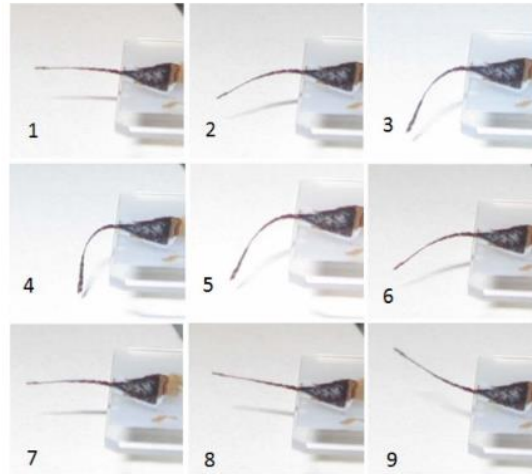


Figure 1.5 - Snapshots of a soft-tissue-paper ferropaper actuator ($0.8 \text{ mm} \times 8 \text{ mm} \times 25 \text{ }\mu\text{m}$) excited by a 46 mT sinusoidal (10 Hz) magnetic field [11].

1.1.3 Electrically responsive actuators

There are many soft, flexible, and stretchable materials capable of converting electrical energy into mechanical energy, such as polymers, gels, liquids, and paper. The electronic signals that drive the actuators allow for rapid and straightforward modulation of signal phase, magnitude, and frequency. In addition, because these actuators are compatible with conventional electronic devices, they can be easily integrated with power devices and electrical drivers [4]. Electroactive polymers (EAPs) are smart materials capable of substantial changes in size or shape subjected to electrical stimulation and can be categorized into two major classes, namely ‘ionic’ and ‘electronic’. The electronic EAPs include electrostrictive elastomers, ferroelectric polymers, and dielectric electroactive polymers (DEAPs), also referred to as dielectric elastomers (DEs), silicone, acrylic, and polyurethane are some examples. The DEAPs are potentially useful materials for actuator applications due to their large actuation strains together with a fast response and a high energy density [12], [13]. The operation of dielectric elastomer actuators (DEAs) is based on Coulombic attraction between two flexible electrodes with a potential difference that is located on separate ends of a compressible membrane, as represented in Figure 1.6.

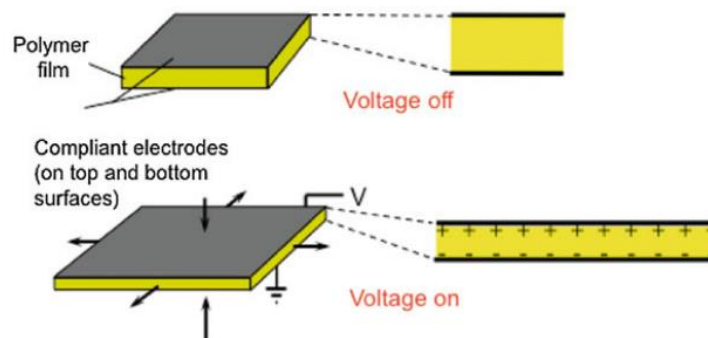


Figure 1.6 - Dielectric elastomer operating principle. When a bias voltage is applied across an elastomer film coated on both sides with compliant electrodes, Coulombic forces act to compress the film in the thickness direction and expand it in plane [14].

When an electric field is applied across the electrodes, the charges pass through an external conducting wire from one electrode to the other. The resulting electrostatic force between the opposite charges on the two electrodes compresses the membrane in thickness. Such compression results in a stretch in the planar area of the membrane. These actuators have rubbery polymer materials with compliant electrodes that have a large electromechanical response to an applied electric field and have been compared to biological muscles in usefulness. Overall performance is highly dependent upon the elastomer stiffness, dielectric constant, and breakdown voltage. The downside to DEAs includes leakage currents and the need for driving voltages on the order of kilovolts, which increases the risk of electrical breakdown [15], [16].

DEAs could be used in different ways, including stacking, folding, framing, inflating, or by rolling them. They can also be bent, expanded or buckled, which increases their range of applications. For instance, Altmüller *et al.* showed large deformations of a soft elastomer membrane using the phase transition of an encapsulated liquid from the liquid to the gaseous state, triggered by an applied electric field. They could do this only using 10 V, as compared to 1000 V typically used in dielectric elastomer actuators. This device was made using polydimethylsiloxane (PDMS) for parts A and B where low-boiling point liquids (water, ethanol and acetone) were injected into the cavity using a syringe [17].

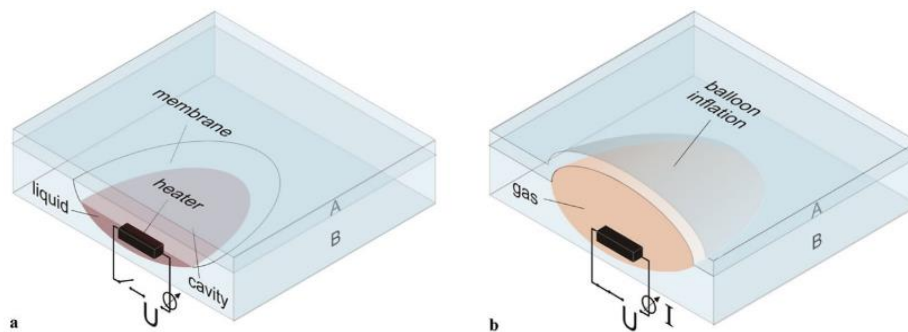


Figure 1.7 - Working principle of the phase change actuator. (a) A cavity within an elastomer is filled with a low-boiling point liquid. Heating of the liquid above its boiling point is achieved with a SMD resistor within the liquid connected to a battery. The cavity is sealed with an elastomer membrane. (b) Upon resistive heating the liquid evaporates and the thin membrane strongly deforms into a balloon shape [17].

After the tests, the highest force (6 N) was achieved with acetone vapour, followed by ethanol with 2.5 N and water with 1.8 N [17].

1.1.4 Pressure-driven actuators

Pressure-driven soft actuators fall under a category of structures known as compliant mechanisms and can be pneumatic or hydraulic [18] actuators. Compliant mechanisms need to pattern their stiffness properties spatially to provide efficient actuation, and they can be stimulated by external forces to generate the desired deformations [3].

In 2016, Gong *et al.* reported the fabrication of a soft rotary actuator based on the peristaltic motion of elastomeric materials, where they used the inflation and deflation of the air-filled bladders in the stator to control the rotation speed of the rotor. They analyzed two configurations, one with an internal rotor for winch/joint-like applications and the other with an external rotor that could be used as a wheel, as Figure 1.8 shows [19].

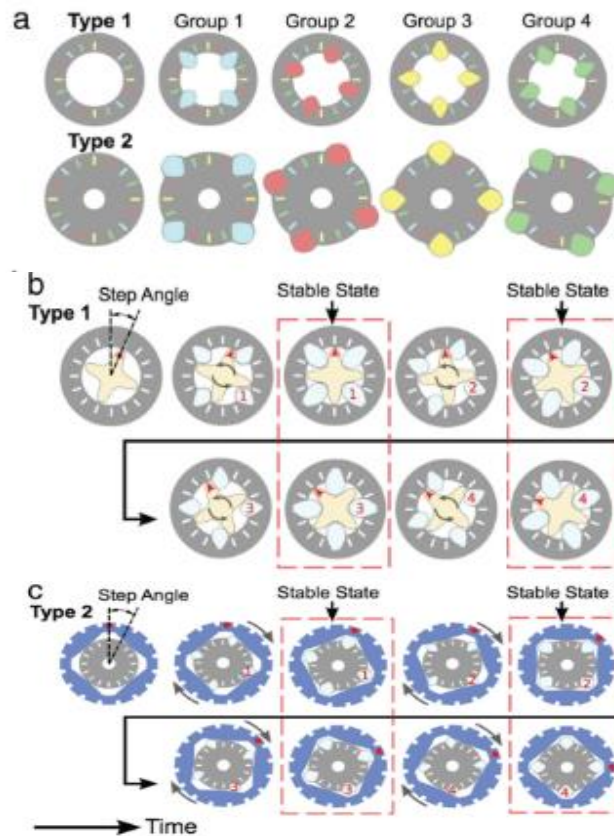


Figure 1.8 - Basic configurations and sequential actuation of subgroups of embedded bladders for two types of rotary actuators. a) Subgroups of bladders inflating around fixed stators in peristaltic fashion (1→2→3→4→1...). Four different colors mark the four subgroups, respectively. b) An actuator with an internal rotor (Type 1) showing a step angle of 22.5°, along with rotation between stable states (enclosed by the dashed lines). c) An actuator with an external rotor (Type 2) showing a step angle of 22.5° and rotation between stable states (enclosed by the dashed lines) [19].

After making different experiments with the actuators, Gong *et al.* showed that type 1 had a faster rotation speed of about 20 rpm but type 2 could bear more external load, reaching 38 mN·m of torque, more six times than the type 1 [19].

One of the most used materials for small-scale elastic fluidic actuators is PDMS, which is typically cast and bonded to create an internal void. Konishi *et al.* created an actuator for cellular aggregate manipulation using a pneumatic balloon actuator (PBA) composed of PDMS. As Figure 1.9 demonstrates, the idea was to create a microfinger using two PBA to manipulate a tiny and sensitive cellular aggregate without causing serious damage [20].

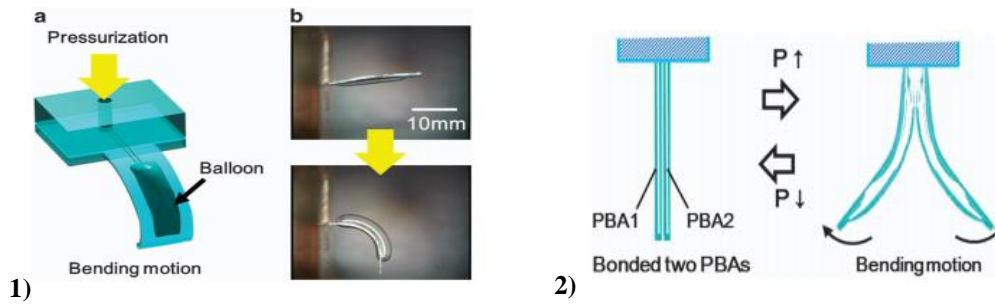


Figure 1.9 – 1) Basic principle of an all PDMS bending PBA consisting of two PDMS films with different thicknesses or material properties: (a) schematics; (b) photographs. 2) A schematic view of the microfingers composed of two opposing PBAs. Normally, closed microfingers that are open due to the bending motion of the PBAs [20].

They were able to fabricate a PBA with $560 \mu\text{m} \times 900 \mu\text{m}$, where the microfingers could pinch a $\phi 200\text{-}\mu\text{m}$ cellular aggregate, using about $30 \mu\text{N}$ of restoring force with no damage [20].

Although a wide range of compatible mechanisms exists, works on high-precision machines and microelectromechanical systems (MEMS) have been well-inspected and reviewed with considerable focus on the topological optimization of continuum structures. Although less popular than thermally and electrically driven nano and microscale electromechanical systems, miniature fluidic pressure-driven soft actuators are gaining traction. These actuators have demonstrated the capacity to produce high forces even at small sizes. However, they usually need to be connected to a quite large external pump [21].

1.1.5 Thermally responsive actuators

Thermally responsive actuators include those activated by infrared (IR), near-infrared (NIR), thermal radiation, and Joule and microwave heating. Joule heating, also known as resistive heating, works by stimulating conductive materials electrothermally. Also, they can be remotely activated by heat application, such as lasers.

Thermal stimulation also provides a safer trigger than UV light or electric field for specific applications such as biomedical applications. However, these actuators tend to be slower and less efficient than actuators using other stimuli [4]. The advantages of thermal actuators are that they have a wide temperature adjustment range, have fast and accurate temperature control, simple structure but have reliable performance. Efforts to increase efficiency and response times include thinner films, more heat absorbent material, and higher power.

Microwaves lay between infrared radiation and radio waves in the electromagnetic spectrum region, ranging from approximately 300 GHz to 0.3 GHz in frequency [22].

In comparison with other electromagnetic waves, microwave possesses better penetrability with a low attenuation degree. Therefore, microwave can be used as a practical controllable remote, environmentally friendly, highly efficient, uniform, and rapid actuation method [23].

Kim, H. *et al* synthesized a new thermo-responsive multifunctional hybrid membrane (HM) through the in situ hybridization of conductive poly(pyrrrole) (PPy) on a photopolymerized poly(N-isopropylacrylamide) (PNIPAm) matrix [24].

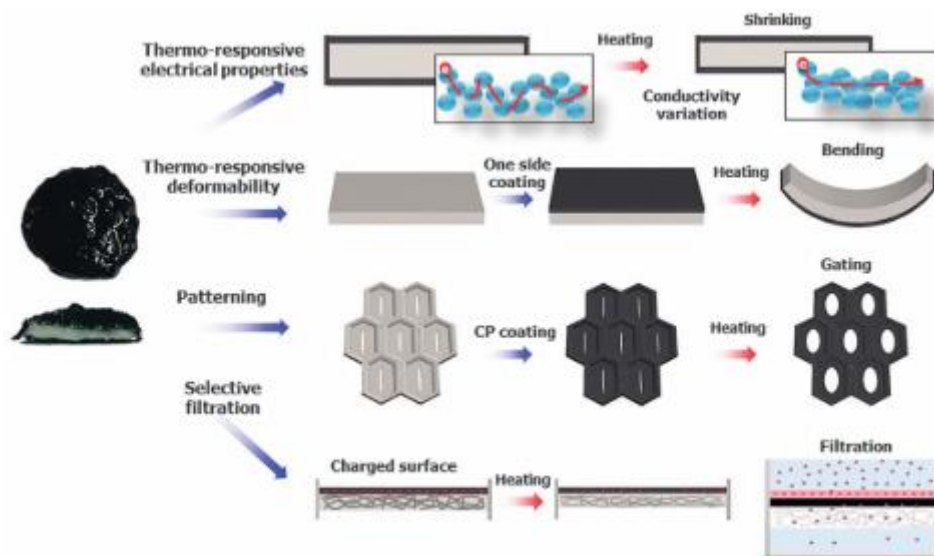


Figure 1.10 - Unique combined features of PNIPAm and PPy provide innovative multiple functions. Thermo-responsive volumetric change induces deformable bending or variation in electrical conductivity. Membranes of various shapes can be fabricated by utilizing photopolymerization patterning. Variation in membrane surface charge can be used for selective filtration of charged molecules [24].

Some plants contain soft materials that confer combined functions of deformability and electrochemical properties. For example, stomata in a leaf have a hydraulic lock function by swelling guard cells in response to ion transport through charged cell membranes. Mimosa rapidly closes their leaves in response to electrical and mechanical stimuli.

The fabricated HM exhibits multiple thermo-responsive functions, including deformability, variation in electrical properties and changes in surface charge. When the PNIPAm and PPy bi-layer actuator is heated above the low critical solution temperature (LCST), 33 °C, it bends or rolls as the pulvinus of mimosa does. When pores are formed in the membrane by utilizing photopolymerization patterning, they possess a gating function with varying electrical potential in response to temperature stimuli, as stomata do. These special properties demonstrate strong potential in the fabrication of bioactuators or soft robots. As volumetric changes caused by thermal stimuli can induce variation in electrical resistance, this functional feature can be utilized as a biosensor. As the surface zeta potential of the HM is changed by thermal stimuli, the electrostatic interaction of charged molecules with the membrane can also be effectively modulated. This functional membrane would be a good candidate for selective filtering of solutions, as the porous membrane of plant roots does. With these multiple functions and a simple yet efficient fabrication process, the present HM has great potential to open a new era of stimulus-responsive hydrogels [24].

Table 1.1 summarizes a brief of the advantages and limitations of the actuators stimulated in different ways.

Table 1.1 - Advantages and limitations of various actuation types.

	External physical stimulation	Advantages	Limitations	Mode of actuation	Ref.
Photo-responsive		Fast response and excellent resolution	Limited deformations	Flapping wing	[25], [26]
		Contactless and noiseless operation	High intensities of light		
Pressure-driven	Pneumatic	Fast and large flexing with low strain	Limited techniques of characterization	Twisting and crawling	[27]
	Hydraulic	Easy to fabricate	Extern components	Gripping	[28]
Magnetically responsive		Highly precise output	Large dimensions	Crawling	[29], [30]
		Fast response	Complex process		
Electrically responsive	Dielectric elastomer	Soft, flexible and stretchable	Slow response	Forward movement	[31]
	Piezoelectric	High energy density	Low payload capacity	Climbing, forward and backward movement	[32]
	Mechanical/ motor	High power-to-weight ratio	Extern components	Crawling	[33]
Thermally responsive	Shape memory polymer	High energy density	Low efficiency	Self-folding	[34]
	Hydrogels	Fast and accurate temperature control	High power consumption	Elongation	[35]

1.2 Pneumatic actuation

Pneumatic soft actuators are a key element for soft robotics due to their inherent simplicity, high forces, and large strokes. However, the necessity of external compressors and pressure-regulating components for hydraulic or pneumatic fluidic actuators limits the size of robots and their applications in highly integrated and mobile systems. Recently, it has been demonstrated that by using phase changes of liquids, pumps can be eliminated in favor of onboard pressure generation. The method is based on the evaporation of a liquid that is placed inside the actuator through heating, usually by electrical power, to obtain the necessary pressure. However, in those examples, power and control have been achieved either by external electrical connections to an off-board power source or using an onboard battery. Batteries and external wire connections obstruct the use of robotic devices significantly, and thus wireless power and control of robotic agents have been a topic of interest recently [36], [37].

Boyvut *et al.* demonstrated the advantages of pneumatic soft actuators using an electrical heater to control a phase change in the internal working fluid, in order to have an ultralow profile, light, wireless soft actuators exhibiting large stroke and high output forces [36].

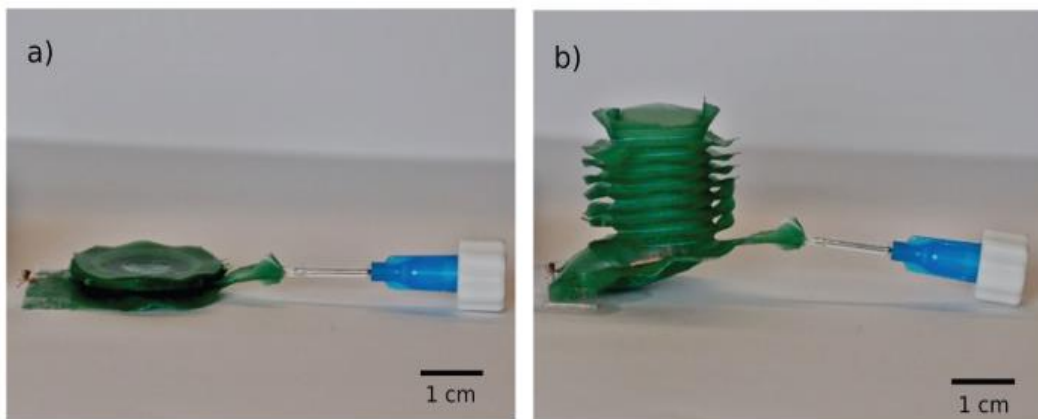


Figure 1.11 - A wireless ultrathin bellows-style actuator before and during actuation. The thicker connection is kept to ease filling by a syringe and is not an essential part of the actuator. a) Before actuation. b) During actuation [36].

The presented actuators use liquid–gas phase change triggered by wireless resonant power transmission and can exhibit ultra-high forces and large expansions in an extremely light and thin form factor. Despite their relatively low speed, a periodic actuation of 15 s, they can find applications in various areas such as biomedical devices, by exploiting the large design space in terms of materials and forms that are compatible with this concept [36].

The present work explores the actuator's stimuli with microwave heat to explore a different approach in the use of the liquid-vapor phase transition in a wireless approach.

1.3 Soft materials for soft actuators

Soft actuators require soft materials that can have high deformation composites that can be activated by external stimuli to generate desired motions and forces/torques. According to the different stimuli, different materials can be used, as is summarized in Table 1.2.

There is a range of soft actuators that are constructed by polymers and gels. This will include synthetic polymers such as silicone rubbers and polyurethanes, as well as some brief mentions of natural polymers, such as DNA or proteins. Similarly, will be also discussed a range of actuators that are created by gels, e.g., hydrogels, oil-based gels, and aerogels. These actuators can use extremely diverse stimuli for actuation, often several at the same time. Another attractive feature for these actuators is that their mechanical properties can be easily programmed through the addition of fillers and the creation of composites during the synthesis process. Because they also have the potential to be lightweight, biocompatible, biodegradable, and easily manufactured, a wide range of polymer- and gel-based soft actuators have been developed. Polymeric materials are attractive for shape programming due to their flexibility, light weight, low price, and compatibility with high throughput processing [38].

Another variety of soft actuators are fluid-based. In general, these actuators can be activated by an increase of pressure, modification of viscosity, and/or selective surface-tension control of the liquid interface. The possibility for fluid manipulation at high speeds and the favorable scaling of surface-tension forces at small sizes make fluid actuators an attractive alternative for some applications. However, in general, fluids have a large number of disadvantages compared to solid-material actuators. For example, fluid-based actuators may not be reproducible as they can be subject to leakage. When pushing an object with a droplet there is a risk of passing, surrounding, or capturing it, which can complicate reliable transportation and deposition. Fluid flows can experience complex dynamics when operating near solid structures and may mix in undesirable ways when operating with or within other fluids. Furthermore, many fluids are also highly dependent on environmental conditions and in small quantities can easily and quickly evaporate. Although these shortcoming can be significant, many can be addressed by encapsulating the fluid in elastic chambers, films, or gels [39].

The commonly used polymers as soft materials include shape memory polymers (SMPs), elastomeric polymers, and electroactive polymers (EAPs). Among these examples, dielectric elastomers, which are a kind of soft electroactive materials, earn special attention for being capable of changes in size and/or shape and also being able to have large actuation strains together with a fast response and a high energy density, as mentioned above.

Soft actuators use flexible materials such as elastomers, which are special polymers that are very elastic. They are lightly cross-linked and amorphous with a glass transition temperature well below room temperature. The intermolecular forces between the polymer chains are rather weak. The cross-links completely contain the irreversible flow, but the chains are very flexible at temperatures above the glass transition, and a small force leads to large deformation. Thus, elastomers have a low Young's modulus and very high elongation at break when compared with other polymers [18], [40], [41].

Simulation and development of paper-based actuators

Nevertheless, actuators that make use of liquid-vapor phase transition usually utilize polymers such as PDMS [42], ecoflex, and sometimes can be used gloves/latex because can easily expand with steam.

Table 1.2 - Materials used for different external stimuli [3], [4].

	Electric field	Magnetic field	Pressure differential	Heat (electro-, photo-thermal, etc.)	Light
Polymers and gels	x	x	x	x	x
Conductive polymers	x			x	x
Liquid-crystal polymers (LCPs), polymer networks (LCNs), elastomers (LCEs)	x			x	x
Ionic-polymer-metal composites (IP-MCs)	x				
Dielectric elastomer actuators (DEAs)	x				
Shape-memory polymers				x	x
Hygromorphic polymers				x	
Ferrogels and ferroelastomers		x			
Hydrogels	x	x	x	x	x
Fluids	x	x	x	x	x
Electrorheological fluid (ERFs)	x				
Magnetorheological fluids (MRFs)		x			
Ferrofluids		x			
Dielectric fluids (electroconjugate fluids (ECFs))	x				
Liquid metals	x	x		x	x
Liquid marbles	x	x			x
Paper (cellulose)	x	x	x	x	
Carbon	x		x	x	
Carbon nanotube (CNT) sheets, yarn	x		x	x	
CNT aerogel	x				

1.3.1 Cellulose actuators

When using thermal actuation by steam generation, an absorbing layer such as a hydrogel is needed. Hydrogels are three-dimensional polymer networks strongly imbibed with water, and the amount of water can approach up to 99 wt.% of the hydrogel mass. Because of this property, hydrogels can considerably swell and shrink (>10 times in volume) when the amount of water in the polymer network changes, which may occur in response to different stimuli such as temperature, light, pH, ionic strength, among others.

Hydrogels are able to act, especially, in aqueous media that, on the one hand, limits their applications but, on the other hand, opens new perspectives for applications where other kinds of actuators are not desirable. For example, various biodegradable and biocompatible stimuli-responsive hydrogels allow the design of actuators for bio-applications. The character of deformation of heterogenous hydrogels can be far more complex and depends on many parameters such as the shape and size of the hydrogel and the character of distribution of heterogeneities [40], [41]. Generally, hydrogels are divided into two categories, according to their origin: biopolymer-based or synthetic. Among the biopolymers, those based on cellulose, which is one of the most abundant on earth, have great potential in hydrogel preparation [43].

Cellulose is the structural component of the cell walls of green plants, constituting about a third of all plant matter. It is a polysaccharide consisting of a linear chain with the formula $(C_6H_{10}O_5)_n$, where $10^2 < n < 10^4$ [44].

The excellent and smart characteristics of cellulosic materials, such as lightweight, biocompatibility, biodegradability, high mechanical strength/stiffness, and low thermal expansion, have made cellulose a high potential material for various industrial applications. Paper is an abundant material that has been used for centuries for printing, packaging, and absorbing liquids. Paper is a porous hydrophilic network of interlinked cellulose fibers. Accorded to the attractive properties of paper, there has been surprisingly little research done on the fabrication of paper actuators [45].

One of the principals uses of cellulose in actuators is as a smart material in the electroactive polymers family, which carries the name of the cellulose-based electroactive paper (EAPap) [46]. There are also paper-based actuators made by incorporating magnetic particles in paper [47] and electrostatic zippers [48]. Then appear different actuators called “Hygroexpansive Electrothermal Paper Actuators” (HEPAs). As Figure 1.12 shows, the actuators are made from paper, conducting polymer, and adhesive tape. The actuators consist of paper with an integrated electrically conducting channel of PEDOT: PSS and thus making a paper/polymer composite that retains the porosity and hydrophilicity of paper. The conducting path, when electrothermally heated, changes the moisture content of the paper by evaporation of the water, contracting the paper, therefore causes actuation [45], [49].

Simulation and development of paper-based actuators

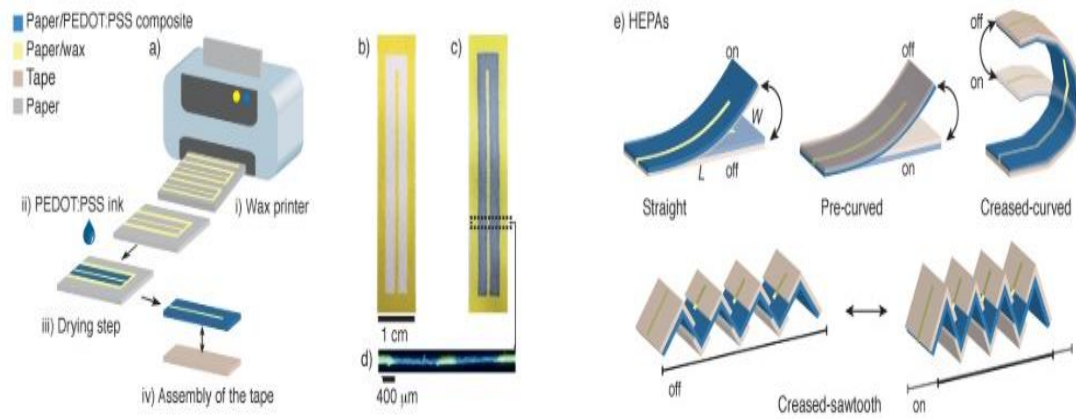


Figure 1.12 - a) Schematic representation of the fabrication of the HEPAs: i) wax is printed and melted into the paper to form the fluidic channels; ii) a suspension of PEDOT:PSS is added to the channels; iii) the water evaporates and deposits the conducting film of PEDOT:PSS in the channel; iv) a piece of tape is attached to the paper/PEDOT:PSS composite to act as a strain-limiting layer. b) Photograph of the wax patterned channel. c) Photograph of the paper/PEDOT:PSS composite. d) Photograph of the cross-section showing that the PEDOT:PSS is embedded in the paper channel. e) Schematic representation of the four HEPAs (straight, precurved, creased-curved, and creased-sawtooth) and their motion of actuation; L , length; W , width [45].

One of the many applications that soft robots can have is the biomedical field. Many biomedical purposes involve delivering biomodified nanoparticles to malignant cells and rapidly heating nanoparticles with an external source such as laser, microwave, ultrasound, or an electromagnetic wave to produce a therapeutic thermal effect or release drugs.

The interaction of nanoparticles with the external source and the subsequent heating effect is fundamental for successfully deploying these innovative techniques. Some metallic nanoparticles used in this area is copper, zinc [50], and gold [51], with special attention for this last one because is the most use. This means that when an external source of heat is pointed to an area with some metallic nanoparticles, the temperature will be higher in the nanoparticles' exact place, making them of great use to kill cancer cells. In actuators, they can be used to provoke a higher temperature in the desired area to maximize the actuation's velocity.

Table 1.3 shows a summary of some thermal actuators where cellulose is used.

Table 1.3 - Paper-based Thermal Actuation

Paper-based Thermal Actuation				
Actuator	Type of thermal actuation	Driving signal	Mode of actuation	Ref.
Photothermal actuated origamis (2020)	Photothermal (IR)	[0-200] mW/cm ²	Self-rolling	[52]
Multiple-stimuli-responsive hydro-gel actuator (2020)	Thermal	[25-360] °C	Swelling/Shrinking/Bending	[53]
Printed paper actuator (2018)	Electrothermal	[40-130] V	Bending	[54]
Shape memory polymer actuator (2018)	Photothermal (IR)	150 W	Bending	[55]
Electrically activated actuators	Electrothermal	20 V, 100 V	Expansion and contraction	[45]
Multiresponsive paper actuator (2016)	Electrothermal	[0-8] V	Bending	[56]

2 Materials and Methods

This chapter briefly reviews the experimental and characterization techniques used in this thesis. First, it is described the preparation of PDMS, polymethyl methacrylate (PMMA) and Ecoflex 30 in order to do thin films through doctor blade. Using UV for surface treatment to assembly the three layers. Secondly, employing a different design and various materials for the fabrication of each layer of the actuator, using a CO₂ infrared laser cutting system for the elastomer (gloves), paper, acetate, and double-sided tape. Lastly, different solutions of metal nanoparticles were impregnated on the paper and to study thermal heat.

2.1 PDMS, PMMA and Ecoflex 30 solutions

For PDMS, was made a solution with SYLGARDTM 184 Silicone Elastomer Base and the corresponding curing agent with a proportion 10:1, respectively, then put to degas for about 30 minutes.

For PMMA, two solutions were produced. One just with PMMA and tetrahydrofuran (THF), using 3 mL of THF for each gram of PMMA, and another also with ethylene carbonate (EC), utilizing 0.3 g for those values. For both solutions, the powders were first weighed, then the THF added and the solution was put right away in the mixer. The solution was covered, so the solvent didn't evaporate quickly, for about 2 hours until it becomes transparent.

Lastly, Ecoflex 30 was achieved by mixing part A and part B, produced by the manufacturer with a ratio of 1:1, for about 10 minutes.

2.2 Doctor Blade

After the solutions were made, it was used doctor blade to create the thin films with different thicknesses, 0.4 and 0.6 mm. For PMMA and Ecoflex 30, the films were made without temperature. For the PDMS the the doctor blade was made with a temperature of 85 °C. Although PMMA's film was deposited in glass, for the others acetate was the better solution. All of the materials were placed with the speed in mode 2. After that, the films of Ecoflex 30 and PDMS needed to dry in the oven at 72 °C for 30 minutes.

2.3 UV

To improve adhesion between PDMS, PMMA and Ecoflex 30, it was made a surface treatment with a Digital UV Ozone System. The samples were placed at 4 cm of the lamp for 40 minutes and then the layers were assembled and put in an hotplate at 70 °C for an hour with a weight on top.

2.4 Laser cutting of layers

Laser cutting was used for more precise patterning of the layers of the actuators. In this procedure was used a pulsed CO₂ infrared laser cutting system (Universal Laser System (ULS) VLS3.5) with a wavelength of 10.6 μm and a focal length of 50.8 mm. The computer-controlled laser system works as a printer where with a vector image input, it is possible to import the desired patterns, previously designed with an image software (Adobe Illustrator CC). These patterns can

encode specific parameters of power, speed, and the number of pulses per inch (PPI), in the form of a Red, Green, and Blue (RGB) color code. In this work, the only parameters that changed were the power and speed to cut each material, as Table 2.1 shows, being that or the acetate was also made some superficial cuts just to make it more bendable.

Table 2.1 - Different power and speed used for which material.

	Power (W)	Speed (m/s)
Acetates	17.5	0.254
Kapton	35	0.178
Acetates (superficial cuts)	8	0.254
Cellophane	5	0.254
Gloves	15	0.254
Papers	12.5	0.254
Double-sided tapes	30	0.203

2.5 Metallic nanoparticles

Different metal nanoparticles (NPs) were used: copper (40 nm), zinc (using two distinct particle sizes: <150 μm and 10 μm), gold and nanowires (NWs) of silver. The gold nanoparticles were produced by e-beam evaporation and deposited a thin layer of 6 nm on top of the paper. This technique consists of applying a current through a tungsten filament which leads to Joule heating and electron emission. High voltage is applied between the filament and the hearth to accelerate these liberated electrons towards the crucible containing the material to be deposited. A strong magnetic field focuses the electrons into a unified beam. Upon arrival, the energy of this beam of electrons is transferred to the deposition material, causing it to evaporate (or sublime) and deposit onto the substrate. The silver nanowires of 5 g/m^2 were added with fibrillated cellulose fibers, placed in the microwave and then dried.

The Cu and Zn solutions were made with a total weight of 1g, with the concentrations of 10 % (w/w), 25% (w/w), 50% (w/w), for copper, zinc (10 μm) and only 10% (w/w) for zinc (<150 μm). After that, 70 μL of each solution was pi-petted into the paper, and the five approaches were tested for 30 seconds and 1 minute in the microwave, one at a time.

2.6 Thermal analysis

A thermal camera is a non-contact device that detects infrared energy (heat) and converts it into a visual image. For this study was used a DIAS Infrared camera that has a precise temperature measurement in the range of -20 $^{\circ}\text{C}$ to 3000 $^{\circ}\text{C}$ and can show images in real-time up to 100 Hz with the thermography software PYROSOFT compact. The samples were tested in the microwave and quickly analyzed.

3 Results and Discussion

In this chapter, the results obtained will be demonstrated and analyzed.

Section 3.1, it is presented some simulations made before the production of actuators.

In section 3.2, it is demonstrated some actuators made similar to those simulated.

While in section 3.3, it is shown the production of the paper-based actuators with different materials.

Lastly, section 3.4 presents the results of the characterization of the metal nanoparticles by a thermal camera.

3.1 Simulation of the actuator

Before fabricating the paper actuators, some simulations, with maximum pressure up to 1 kPa as stimulus, were made using LiveLink™ for MATLAB®, COMSOL Multiphysics® software, where were utilized PDMS, acrylic, PMMA and Ecoflex 30 as materials. These results were obtained by Prof. Aaron Mazzeo in preparation for this Master's thesis that was supposed to be carried out at Rutgers University, NJ, USA. This model assumes that the deformation suggested in the simulations is only caused by an increase in pressure, which in real situations would be caused by steam generation. Heat (i.e. temperature rise) was not taking into account, which means that effects occurring in real situations such as thermal expansion/contraction and stress generated between layers, for instance, is not considered.

In the first model, two layers of PDMS with a thickness of 0.1 mm and 1 mm were used on the upper surface, while acrylic with a thickness of 1 mm was used for the lower layer. Figure 3.1 demonstrates the deformation of the actuator at these parameters with a total displacement of 1 mm in the middle when the pressure in the bladder reaches 1 kPa.

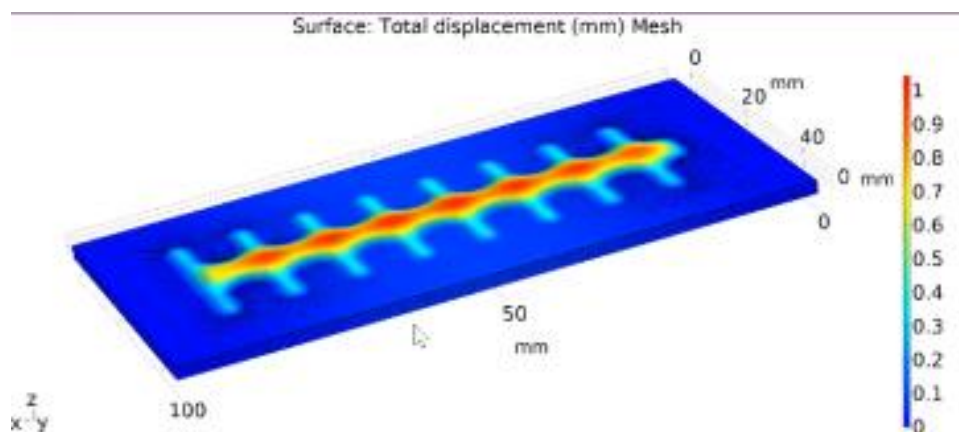


Figure 3.1 - First design of simulation, an actuator using PDMS and acrylic as materials and having a maximum displacement of 1 mm in the red area, obtained with pressure.

Simulation and development of paper-based actuators

Another design was developed using Ecoflex 30 (0.2 mm) on the top layer following the Yeoh model [57], while a patterned PDMS/PMMA laminate was used for the bottom layer (0.1 mm) to facilitate the mechanical action of actuation, as shown in Figure 3.2.

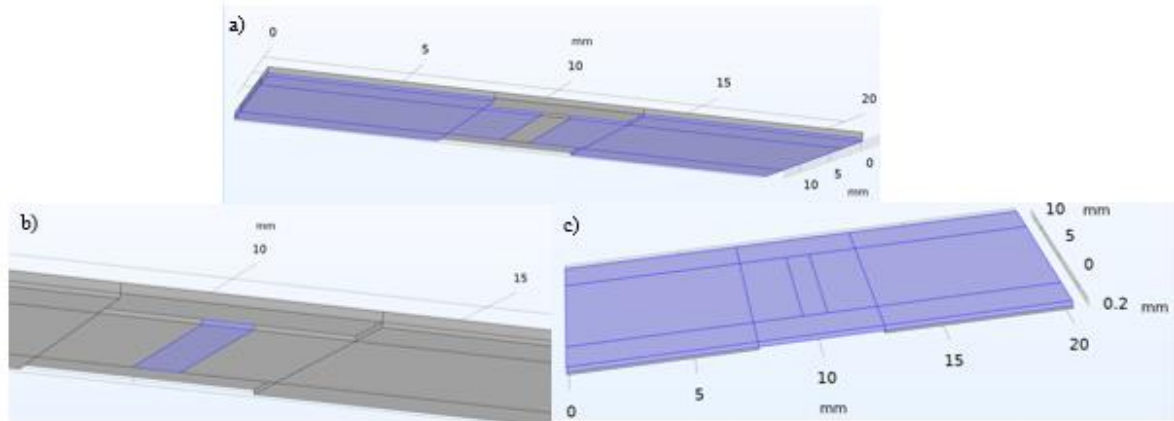


Figure 3.2 - Another design of an actuator assembled with a) the PMMA layer, b) the PDMS layer and c) the layer of Ecoflex 30.

In this configuration, the pressure causes a bladder on the Ecoflex 30, which consequently causes the actuator to bend, resulting in some movement, as depicted in Figure 3.3. A maximum pressure of 1 kPa was simulated in the joint, with the formation of the bladder, achieving a displacement of 1.3 mm at about half pressure (Figure 3.3 a)) and reaching an expansion of near 3 mm with full pressure (Figure 3.3 b)), which led it to bend more significantly when the bladder was smaller.

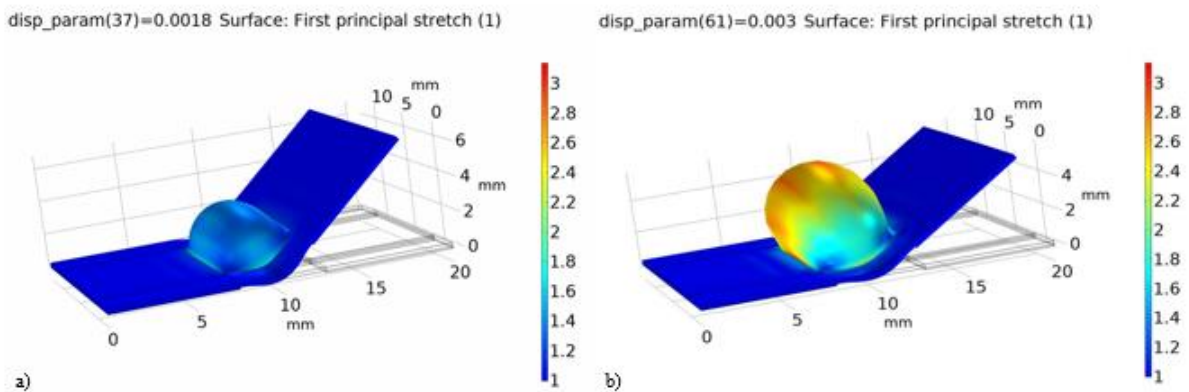


Figure 3.3 - The simulation of the actuator with the layout in the picture above, using Ecoflex 30 on the bottom, PDMS and PMMA on top. a) a pressure of about 0.6 kPa was applied leading to a displacement of about 1.3 mm, while when b) a pressure of 1 kPa is reached in the joint with PDMS to form a bladder with a maximum stretch of near 3 mm.

Next, the behaviour of a more complex actuator was simulated, based on the actuator represented in Figure 3.3. However, instead of one actuator, four actuators were simulated, all connected in such a way that they could represent a small robot, as Figure 3.4 illustrates.

In this model, the observed displacement (1.3 mm) was the result of the same pressure used for the results in Figure 3.3 a). With this simulation, it was stated that four interconnected actuators could perform as well as just one and this assembly could be used as a robot in locomotion.

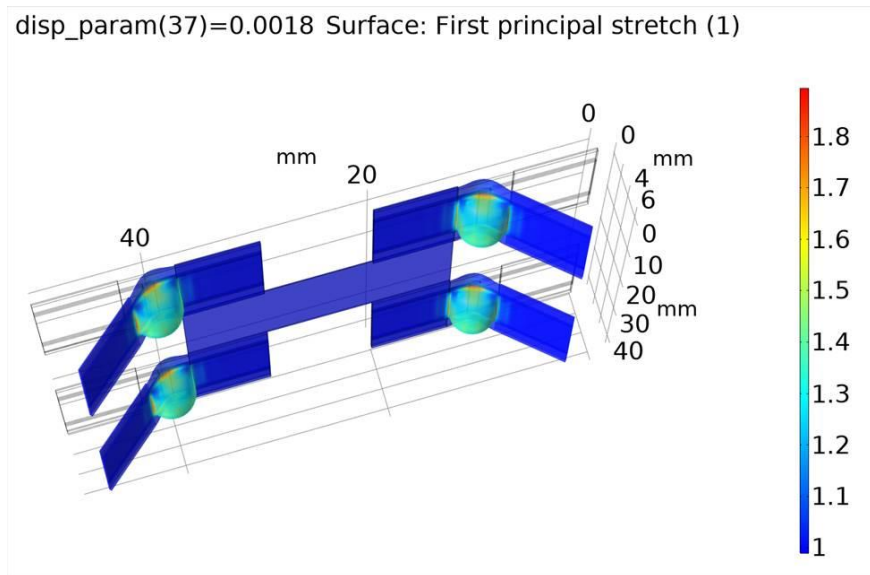


Figure 3.4 - Four actuators put together, operating at the same time, to form a small robot, using pressure to obtain a maximum stretch of 1.3 mm.

3.2 Production of the simulated actuator

After running the simulations, the design shown in Figure 3.2 was applied to real actuators because was more promising to get better results. Figure 3.5 shows how the assembly of the layers was done. For practical reasons, the PDMS film was chosen slightly larger than in the simulation to ensure a good seal.

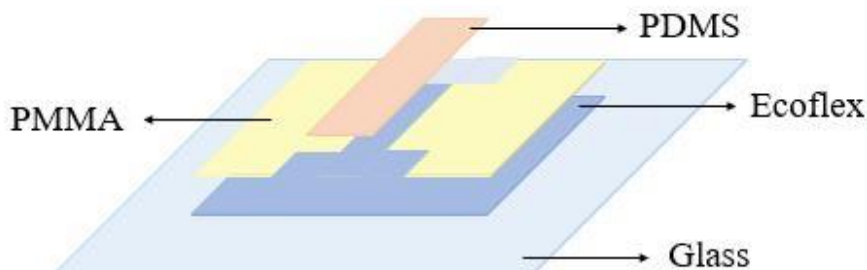


Figure 3.5 - Structure of the actuators made according to the structure used in the simulation made with Ecoflex 30 (40x20 mm), PMMA (19 x 20 mm) and PDMS (6 x 20 mm).

Films of Ecoflex 30, PMMA and PDMS were prepared by doctor blade with different thicknesses. It was verified that for PMMA and Ecoflex 30, 0.6 mm resulted in a more effective approach as it allowed mechanically stable films. For PDMS, the best compromise was obtained at 0.4 mm. After drying, the final thickness was: Ecoflex 30: 0.382 mm; PMMA: 0.114 mm and PDMS: 0.248 mm. For PMMA, two solutions were produced, one with EC and the other without. The film with EC had a higher modulus of elasticity but resulted in a lower elongation at break, which could affect its use in actuators. The layers were then cut with a bistoury and arranged according to the structure in Figure 3.2. Figure 3.6 shows some of the replicated actuators.

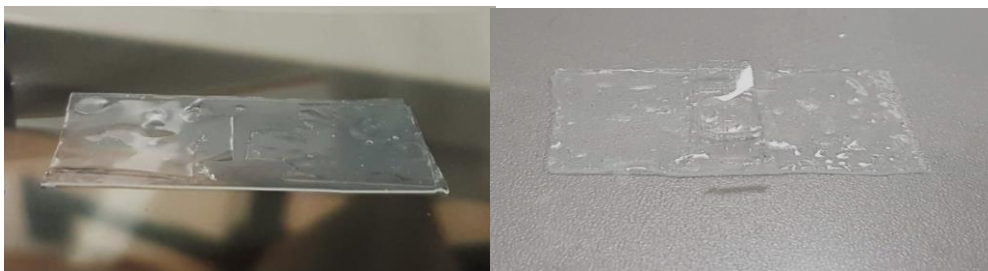


Figure 3.6 – Some examples of the actuators made with Ecoflex 30, PMMA and PDMS with different thicknesses.

After choosing the right materials and thicknesses, the next step was to assemble the layers. It was verified that there was no adhesion between them, especially with PDMS and Ecoflex 30, and it became becoming clear that a surface treatment would be required. Some practical options could be atmospheric plasma [58] or UV Ozone exposure [59]. Figure 3.7 illustrates some of the various experiments with UV treatment. It was found that this treatment was only effective for PDMS, but not for improving adhesion between all layers.



Figure 3.7 – Experiment of the adhesion between PDMS and Ecoflex 30 after UV treatment: 1) both PDMS and Ecoflex 30 with UV; 2) only Ecoflex 30 with UV; 3) only PDMS with UV; 4) PDMS and Ecoflex 30 with UV and PMMA between them without treatment.

Since the UV treatment did not work as good as expected, polyvinyl alcohol (PVA) [60] was still tested to bond the layers in a simple way. In this case, a solution of EVO-STIK Evo-Bond Waterproof PVA with water in a 3:2 ratio by volume was used. The solution was used between the layers and dried for about 24 hours.

As the attempts to assemble the three layouts did not work, it was decided to continue the experiments with the other materials. These results allowed to understand that the simulation had to take into account many more critical parameters than the mechanical properties of the layer.

3.3 Paper-based actuators

After the first simple simulation, the same designs were applied to real actuators. However, these actuators were produced with different materials mainly because the goal was to create an actuator that worked by generating steam and therefore requiring a layer that could retain water inside it (paper was used for this purpose). At the same time, some problems arose in the integration of the materials used for the simulation. Nevertheless, the materials selected for the real actuators have similar Young's Modulus to those used in the simulation, as indicated in Table 3.1. Latex or nitrile were used for the actuator design instead of PDMS and Ecoflex 30, and acetate sheets were used as an alternative to polymethyl methacrylate (PMMA).

Table 3.1 - Indication of Young's Modulus for which material, according to the literature [61]–[64].

	Young's Modulus
Latex	0.6 MPa
Nitrile	4 MPa
PDMS	0.8-3 MPa
Ecoflex 30	0.17 MPa
Acetate sheet	2.4 GPa
PMMA	1.8-3.1 GPa

In this section, all actuators were tested on the microwave at a power of 800 W and for 1 minute. After several tests, this was the time when most of the actuators started to show some movement. During the tests, a glass of water was also placed in the microwave to absorb some of the radiation and not damage the device.

Observing the actuators while they were moving was a complicated process because it was not possible to record what was happening inside the microwave oven. Therefore, the only way to analyze the actuator was to look through the door of the microwave oven, which was not very visible because of the black sheet protecting us from radiation.

Initially, the first design simulated was tested using latex, Whatman paper n°1 (porous filter paper) embedded in water, and then tape to connect all the layers. Figure 3.8 shows how the setup was done for this design. Only one of the tests had some actuation (Figure 3.9) involved placing the paper on top of the latex, then the water (with red dye) on top of the paper, and finally the tape on top of that.

Simulation and development of paper-based actuators

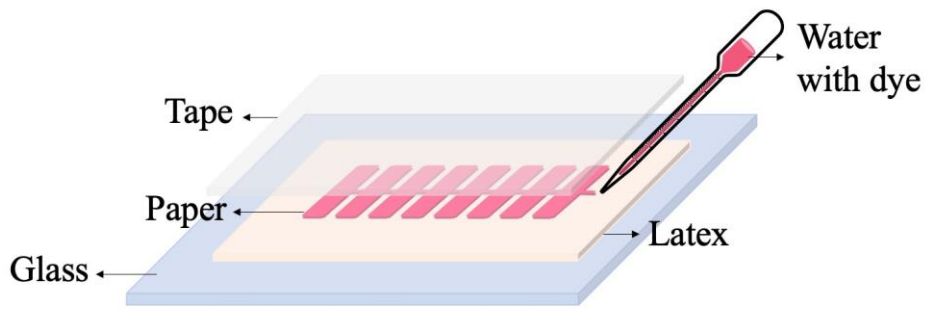


Figure 3.8 – Assembly of the first actuators made according to the structure used in the simulation made with latex, paper soaked in water and tape on top.



Figure 3.9 - Actuator tested during 1 minute in the microwave oven at 800 W.

As the second simulation's design was more promising, after the initial experiments, another shape for the actuators was conceived with the size of (2.5 x 5.6) cm, as presented in Figure 3.10. For this layout, acetate was used as the stiffer part with some superficial grooves to make it more bendable in the joint. Then, a frame of double-sided tape was used to join all the layers together, having an aperture in the middle being exactly the same size as the paper. Finally, the latex was used as a flexible material to form the bladder.

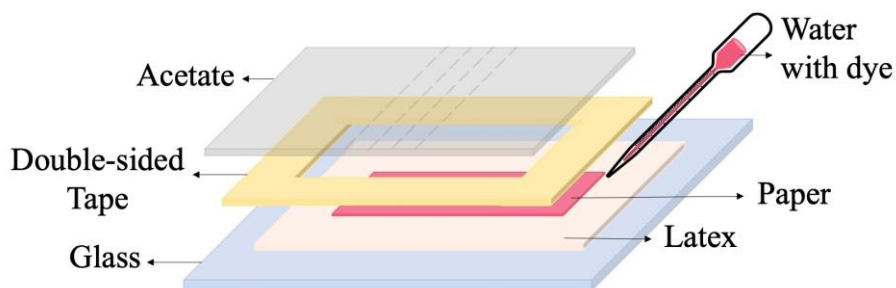

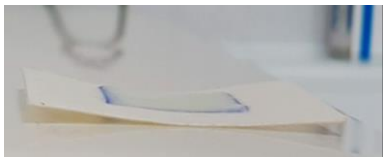
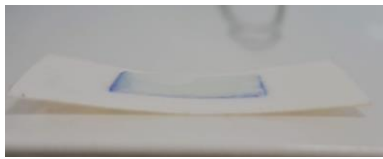
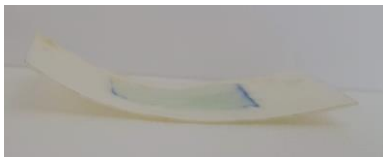




Figure 3.10 – Structure of the second actuator, using latex, double-sided tape, paper with water and acetate with superficial cuts in the middle to be more flexible.

Simulation and development of paper-based actuators

First, different volumes of water were tested to define the correct volume for the actuator so that it neither dry out nor overflow. As shown in Table 3.2, the volumes varied between 50 μL and 90 μL .

Table 3.2 – Experiment of different volumes of water in the actuators.

50 μL		
70 μL		
90 μL		
Soaked in water		



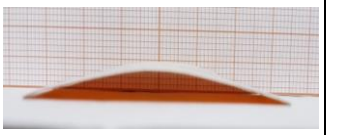





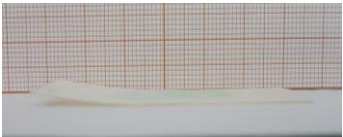
When the actuators were analyzed after microwave irradiation, those where the paper was moisturized with 50 μL and those that were completely soaked with water, showed no movement. The first one did not have enough water so the paper was too dry, while for the last some water that spilled out in the assembly caused slight delamination of the latex. Although the actuators moisturized with 70 μL and 90 μL had shown some movement, the actuator with 90 μL for an area of 3 cm^2 showed better response. Therefore, a water volume of 90 μL was adopted for the following experiments.

After reaching the optimal water volume, several double-sided tapes were analyzed as well as another type of elastomer (nitrile), all with different thicknesses. Table A.1, in annex, illustrates below, the double-sided tape with 209 μm was the one that performed better compared to the other tapes, although the thickness was almost five times higher. The results obtained suggested that the thickness of the double-sided tape did not have a significant impact. This is attributed to the fact that it is only present in the frame of the actuators. Although both actuators had latex and nitrile, the nitrile glove appears to shrink when heated, resulting in undesirable behavior of the actuator.

After examining the double-sided tape and the elastomer, the last step was to analyze the rigid part and the paper. Neither significant expansion nor contraction was expected for the acetate sheet. Cellophane and Kapton were also tested since they are also flexible, thin and have good steam and water insulation.

As it is observable in Table 3.3, the cellophane exhibited a very different release movement than expected and this material was discarded. It proved to be too thin to provide mechanical stability assuming issues not considered in the simulations such as differential thermal expansion/contraction.

Table 3.3 - Results of testing acetate, cellophane, Kapton, properties of porous paper and different kinds.





	Acetate (101 μm)	Cellophane (17 μm)	Kapton (79 μm)
What-man paper n°1 (181 μm)			
What-man paper (86 μm)			
What-man paper (80 μm)			
Soft Tissue (134 μm)			
Soft Tissue (56 μm)			

The papers differed in thickness and hydrophobicity, with the 86 μm , 80 μm and the 181 μm paper having the highest to lowest hydrophobicity. It was also tested soft tissue paper with 56 μm and 134 μm , as *Ding, Z. et al.* demonstrated to be the better for their actuator [11]. However, in our experiments, the Whatman paper performed better, which can be attributed to the controlled moistening that was adopted in this work.

The best results were obtained for the 181 μm and 80 μm paper, those that are more hydrophilic, promoting better moistening.

Further tests were carried out to see which paper had a greater impact in the motion of the actuator, as Table 3.4 shows. The one that more constantly demonstrates bigger movement is the actuator with Whatman paper n°1 (181 μm thick).

Table 3.4 – Results testing between Whatman paper n°1 (181 μm) and whatman paper (80 μm).

	Whatman paper n°1 (181 μm)	Whatman paper (80 μm)
1° test		
2° test		

Once the best materials were known, they were applied in different designs, changing only the size of the area to be inflated (areas between 1.44 and 4.75 cm^2), as shown in Figure 3.11.

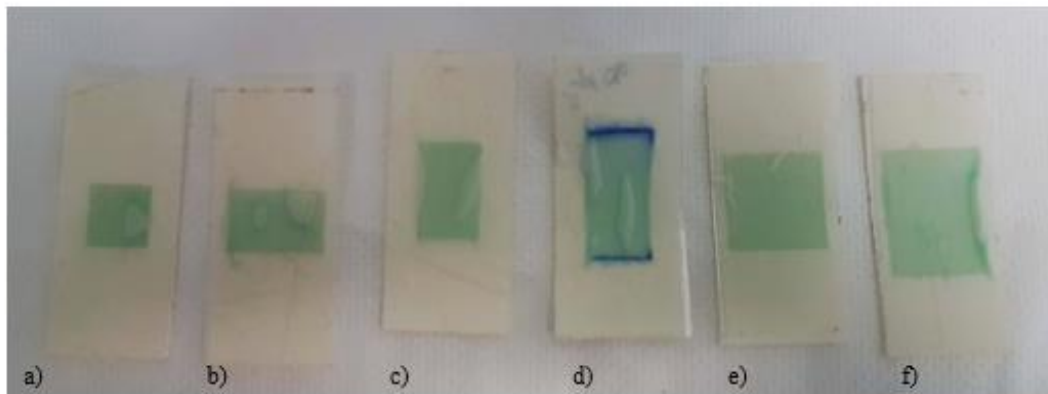


Figure 3.11 – Different areas of the inflated zones. a) 1.44 cm^2 ; b) and c) 2.28 cm^2 ; d) 3 cm^2 ; e) 3.61 cm^2 and f) 4.75 cm^2 .

All designs were tested considering the volume of water proportional to the area, taking into consideration the volume defined previously of 90 μm for an area of 3 cm^2 . The actuators shown in Figure 3.11 b), e) and f) were the first to be excluded, as the straight line between the paper and the end of the actuator provokes a path for air to escape when the latex is pulled off. The one in Figure 3.11 a) was also set aside because the area was too small. Only those in Figure 3.11 c) and d) had some actuation, with d) being more noticeable than the previously used design.

Then, the best actuator, made of acetate sheet (101 μm), double-sided tape (209 μm), Whatman paper n° 1 (181 μm) and latex glove (85 μm) with an area of 3 cm^2 was observed with the thermal imaging camera, right after being tested in microwave oven for 1 minute, reaching a temperature of 74.1 $^{\circ}\text{C}$, as shown in Figure 3.12. The temperature achieved inside the microwave was close to 100 $^{\circ}\text{C}$, which could be sufficient for a phase change from liquid to vapour.

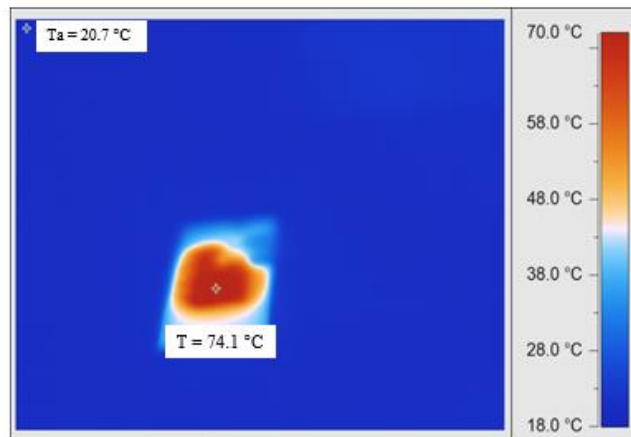


Figure 3.12 – Thermal image of the actuator that had the most significant motion.

3.4 Thermal analysis

In some studies, metallic nanoparticles are used to kill cancer cells when an external source is pointed to where they are located, this cause a local temperature increase. Having in mind the concept of localized heating, it was studied the influence of metallic nanoparticles incorporation in the paper (copper, zinc, gold and silver) and how they could improve the ability to enhance the temperature faster and to higher values in order to maximize the actuation velocity.

Seven aqueous solutions were prepared (Figure 3.13 a): three of copper with a particle size of 40 nm (concentrations: 10% (w/w), 25% (w/w) and 50% (w/w)), three of zinc with a particle size of 10 μm (concentrations: 10% (w/w), 25% (w/w) and 50% (w/w)) and another of zinc nanoparticles, with a size smaller than 150 μm . it was only made with a concentration of 10% (w/w).

The gold nanoparticles were produced by e-beam evaporation and deposited a thin layer of 6 nm on top of the paper. The silver nanowires of 5 g/m^2 were added with fibrillated cellulose fibers, placed in the microwave and then dried. For an area of 3 cm^2 , the paper contained 1.5 mg of silver nanowires. In Figure 3.13 b) and c) it is shown paper with metallic nanoparticles, gold and silver, respectively.



Figure 3.13 – a) The solution of the metallic nanoparticles: copper 40 nm; zinc 10 μm and zinc <150 μm ; b) paper with gold nanoparticles and c) silver nanowires with fibrillated cellulose fibers.

The actuators were assembled with the paper impregnated with 70 μL of the solutions of metallic nanoparticles, as in Figure 3.14 a). For the paper with gold and silver (Figure 3.13 b) and c)), they were placed with adjacent wet paper, as in Figure 3.14 b). After, they were tested for 30 and 60 seconds each, where the temperature was observed through the thermal camera. It was tested the temperature of an actuator just with water to compare (already shown in Figure 3.12).

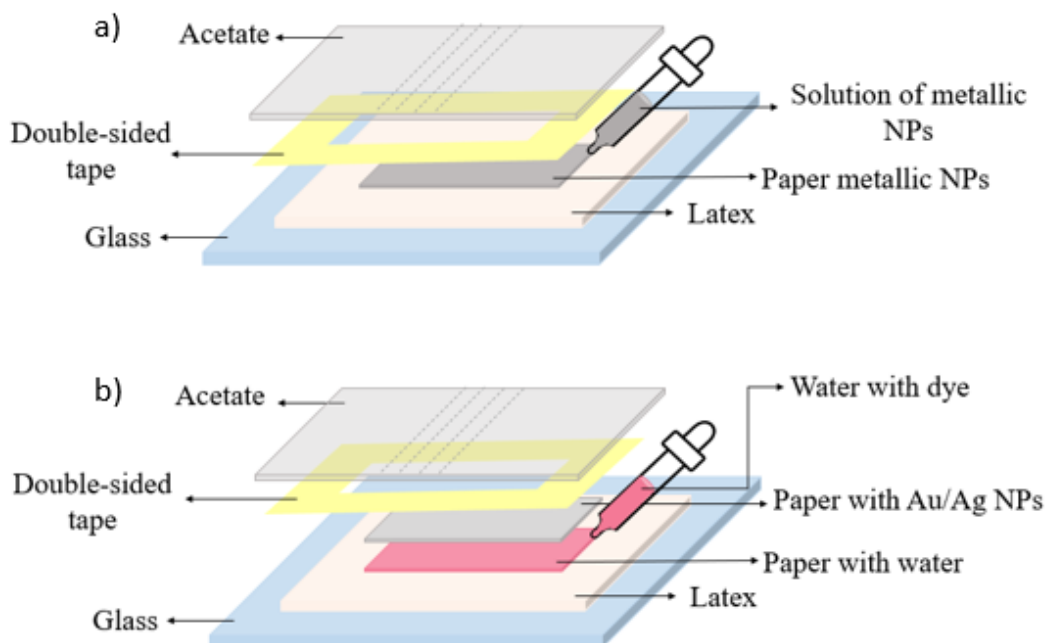



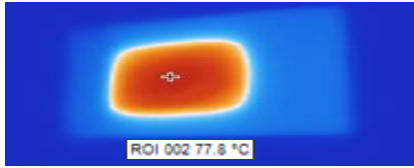
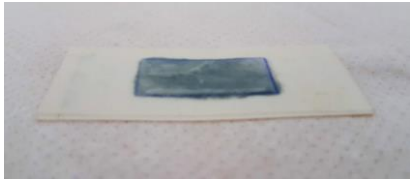
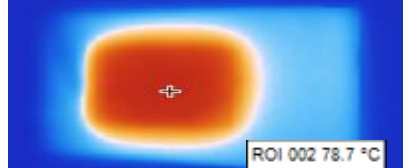
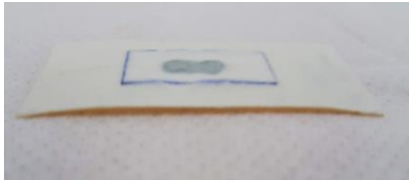
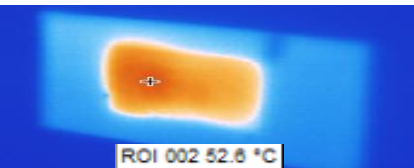
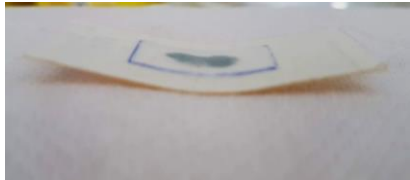
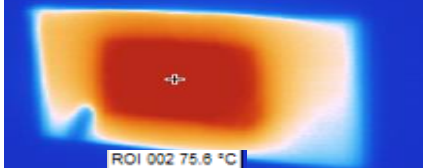
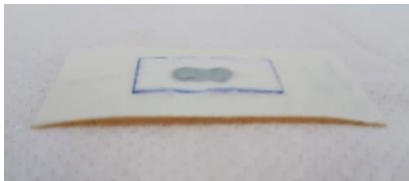
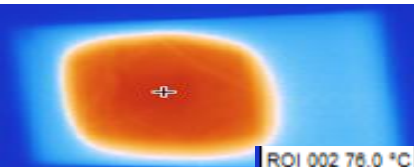
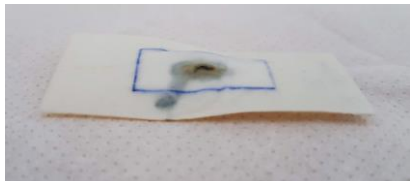

Figure 3.14 – Structure similar as in Figure 3.10: a) with a solution of metallic nanoparticles; b) paper with Au/Ag nanoparticles with adjacent wet paper.

In first place, the actuators with nanoparticles of zinc (10 μm) were submitted to experiment. Table 3.5 illustrates that the temperature increases for different exposure time and different metal nanoparticles concentration. However, a higher temperature does not correspond directly to faster actuation.

In general, and since the measurements are made already outside the oven, it was not observed a significant temperature increase in the presence of zinc nanoparticles. This is just a qualitative indication and does not mean that some differences indeed occur when the actuators were inside the oven.

Simulation and development of paper-based actuators

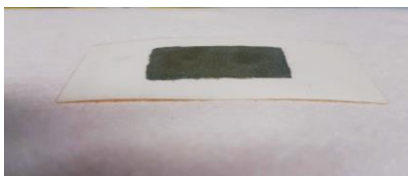
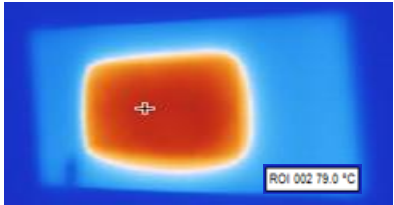
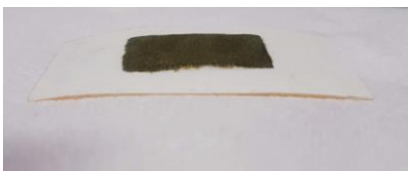
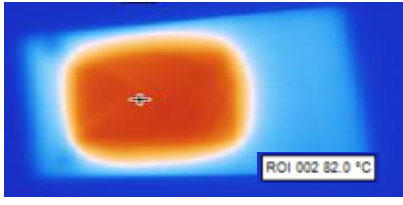
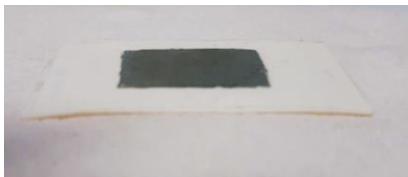
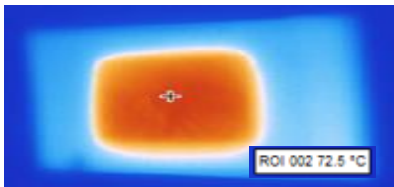

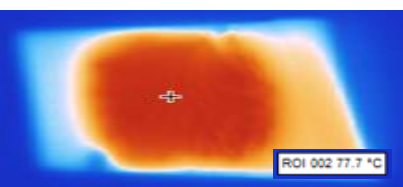
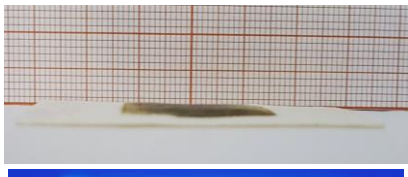

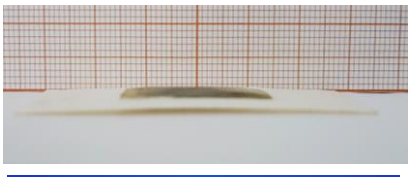
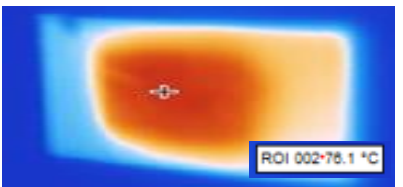
Table 3.5 - Results by thermal camera and movement of actuators made with zinc ($10\ \mu\text{m}$) for different concentrations and times.

	30 seconds	60 seconds
Zinc ($10\ \mu\text{m}$) 10% w/w	 	 
Zinc $10\ \mu\text{m}$ 25% w/w	 	 
Zinc $10\ \mu\text{m}$ 50% w/w	 	 

For copper (Table 3.6) again no major differences in the temperature measured were observed, when comparing with paper soaked with water without nanoparticles. The temperature measured for the actuator that showed some motion was around $77.7\ \text{°C}$, $3.6\ \text{°C}$ more than without nanoparticles (not considered yet to be evidence of the direct benefit of the nanoparticles).

Simulation and development of paper-based actuators

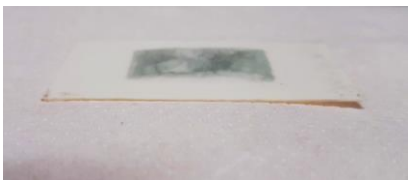

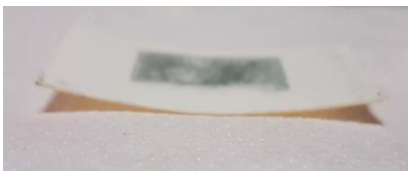
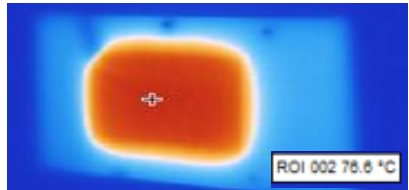
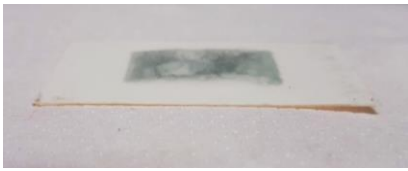
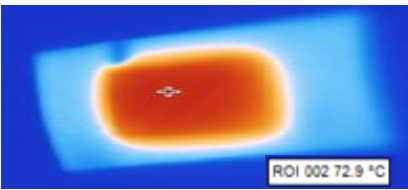
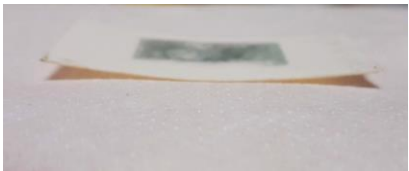

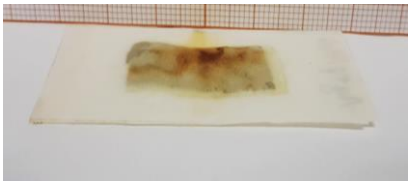
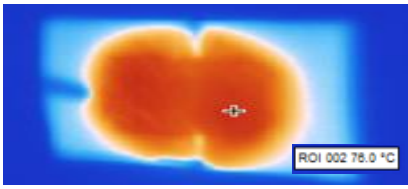
Table 3.6 - Results by thermal camera and movement of actuators made with copper 40 nm for different concentrations and times.

	30 seconds	60 seconds
Copper 40 nm 10% w/w	 	 
Copper 40 nm 25% w/w	 	 
Copper 40 nm 50% w/w	 	 

In Table 3.7, it is shown the actuators where the paper was moisturized with nanoparticles of zinc (<math><150 \mu\text{m}</math>) and the actuators that have paper with gold and silver nanoparticles. The ones with solution of zinc nanoparticles (<math>< 150 \mu\text{m}</math>) and the paper with gold nanoparticles exhibited some actuation and presented a temperature of 76.6 °C and 76.8 °C, more 2.5 °C and 2.7 °C than without nanoparticles, respectively.

Simulation and development of paper-based actuators

Table 3.7 - Results by thermal camera and movement of actuators made with zinc <math>< 150 \mu\text{m}</math>, gold nanoparticles and silver nanowires for different times.

	30 seconds	60 seconds
Zinc <math>< 150 \mu\text{m}</math> 10% w/w	 	 
Paper with gold nps 6 nm film	 	 
Paper with silver nws 1,5 mg	 	-

In this case, although the temperature could increase with the concentration of metallic nanoparticles for zinc (10 μm), this was not a trend for all the metallic nanoparticles. This suggests the introduction of the nanoparticles did not have a relevant impact in improving the steam generation in the actuators. This may be due to insufficient concentration of metallic particles and/or the not optimal dimension of the particles to interact with the microwave wavelength radiation.

Table 3.8 shows a summary of actuator temperatures by thermal analysis with and without metallic nanoparticles for different times.

Table 3.8 – Summary of actuator temperatures by thermal analysis with and without metallic nanoparticles for different times.

	30 seconds	60 seconds
Without NPs	78 °C	74.1 °C
Zinc (10 µm) 10% w/w	77.8 °C	78.7 °C
Zinc 10 µm 25% w/w	52.6 °C	75.6 °C
Zinc 10 µm 50% w/w	76.0 °C	116.5 °C
Zinc < 150 µm 10% w/w	70.7 °C	76.6 °C
Copper 40 nm 10% w/w	79.0 °C	82.0 °C
Copper 40 nm 25% w/w	72.5 °C	77.7 °C
Copper 40 nm 50% w/w	77.7 °C	76.1 °C
Paper with Au NPs 6 nm film	72.9 °C	76.8 °C
Paper with Ag NWs 1,5 mg	76.0 °C	-

In overall, the NPs lead to an increasing of the temperature for the heating time of 60 s, representing an heating of 8.4 °C in average.

However, the copper 40 nm and zinc 10 µm, for a concentration of 25% w/w, NPs were the ones with the most promising results, leading to an increasing of 3.6 °C and 1.5 °C, respectively, compared to the actuators without nanoparticles.

4 Conclusion and Future perspectives

The main goal of this thesis was to make a small review of the field of soft actuators, an area under development. The option for making a review came from the impossibility of going to the lab of Prof. Aaron Mazzeo at Rutgers University, where this master thesis work was supposed to be performed. In order to keep on this interesting topic, it was decided to move for a revision-thesis, but combining with some experimental results on some exploratory work that could be performed in the labs at CENIMAT/CEMOP. The focus was on simulate and develop paper-based actuators in a way never made before, using steam as a working fluid heated with microwaves to inflate bending joints/bladders.

In the preparation of the actuators with PDMS, PMMA and Ecoflex 30, the assembly of these three layers revealed to be challenging because of the lack of adhesion even with surface treatments.

During the development of paper-based actuators, many tests were made, where it was possible to analyze the better materials and design. Despite the material and design selection, one of the problems was the replication of the same actuator several times and have constant actuation, which may be related to the different tensions of the elastomers when assembling the layers. Also, some impurities in the materials or even the weather can affect the water's evaporation. Still, the preliminary results obtained during this work, gave some hints about the next steps and allowed to get some conclusions.

From the different designs tested, the actuator with better results was made with latex, Whatman paper n°1, acetate's sheet, and double-sided tape. Correspondingly, which material as 85 μm , 181 μm , 101 μm , and 209 μm , with a total thickness of 576 μm . This actuator shown actuation but also reached a temperature of 74.1 $^{\circ}\text{C}$.

One of the difficult parts was the impossibility to see the actuation taking place and not being possible to characterize the bending of the actuator. Therefore, the evaluation of the actuator response under a microwave stimulus, was made after opening the oven. It is possible that the actuation observed is lower than the real one reached inside the microwave oven during the heating process.

It was tried to an approach to promote the local heating of the actuator to maximize the actuator's velocity. For this, it was made a study of thermal heat of metallic nanoparticles on paper, using copper, zinc, gold and silver nanoparticles. The Cu NPs, solution with a concentration of 25% (w/w), had the best results, being possible to increase the localized temperature of the paper when compared with the paper without the nanoparticles (maximum temperature 74.1 $^{\circ}\text{C}$), reaching a temperature of 77.7 $^{\circ}\text{C}$ when 70 microliters were deposited on the paper.

In the future it would be interesting to make a surface treatment with an atmospheric plasma for PDMS and Ecoflex 30 in order to improve the adhesion between them, create an actuator that can return to the original position and that could be used more than one time, test with other materials with less thickness and better encapsulation hability.

References

- [1] F. Iida and C. Laschi, "Soft robotics: Challenges and perspectives," *Procedia Comput. Sci.*, vol. 7, pp. 99–102, 2011.
- [2] M. Manti, V. Cacucciolo, and M. Cianchetti, "Stiffening in soft robotics: A review of the state of the art," *IEEE Robot. Autom. Mag.*, vol. 23, no. 3, pp. 93–106, 2016.
- [3] L. Hines, K. Petersen, G. Z. Lum, and M. Sitti, "Soft Actuators for Small-Scale Robotics," *Adv. Mater.*, vol. 29, no. 13, 2017.
- [4] N. El-Atab *et al.*, "Soft Actuators for Soft Robotic Applications: A Review," *Adv. Intell. Syst.*, vol. 2, no. 10, p. 2000128, 2020.
- [5] G. M. Whitesides, "Soft Robotics," *Angew. Chemie - Int. Ed.*, vol. 57, no. 16, pp. 4258–4273, 2018.
- [6] H. Tian, Z. Wang, Y. Chen, J. Shao, T. Gao, and S. Cai, "Polydopamine-Coated Main-Chain Liquid Crystal Elastomer as Optically Driven Artificial Muscle," *ACS Appl. Mater. Interfaces*, vol. 10, no. 9, pp. 8307–8316, 2018.
- [7] K. Kumar, A. P. H. J. Schenning, D. J. Broer, and D. Liu, "Regulating the modulus of a chiral liquid crystal polymer network by light," *Soft Matter*, vol. 12, no. 13, pp. 3196–3201, 2016.
- [8] T. Sakai *et al.*, "Photoresponsive slide-ring gel," *Adv. Mater.*, vol. 19, no. 15, pp. 2023–2025, 2007.
- [9] T. K. Mudiyansele and D. C. Neckers, "Photochromic superabsorbent polymers," *Soft Matter*, vol. 4, no. 4, pp. 768–774, 2008.
- [10] K. Ichimura, S. K. Oh, and M. Nakagawa, "Light-driven motion of liquids on a photoresponsive surface," *Science (80-.)*, vol. 288, no. 5471, pp. 1624–1626, 2000.
- [11] Z. Ding, P. Wei, G. Chitnis, and B. Ziaie, "Ferrofluid-impregnated paper actuators," *J. Microelectromechanical Syst.*, vol. 20, no. 1, pp. 59–64, 2011.
- [12] Z. Zhao, C. Shuai, Y. Gao, E. Rustighi, and Y. Xuan, "An application review of dielectric electroactive polymer actuators in acoustics and vibration control," *J. Phys. Conf. Ser.*, vol. 744, no. 1, 2016.
- [13] J. Kim, J. W. Kim, H. C. Kim, L. Zhai, H. U. Ko, and R. M. Muthoka, "Review of Soft Actuator Materials," *Int. J. Precis. Eng. Manuf.*, vol. 20, no. 12, pp. 2221–2241, 2019.
- [14] L. Rasmussen, *Electroactivity in polymeric materials*, vol. 9781461408. 2012.
- [15] J.-H. Bae and S.-H. Chang, "PVDF-based ferroelectric polymers and dielectric elastomers for sensor and actuator applications: a review," *Funct. Compos. Struct.*, vol. 1, no. 1, p. 012003, 2019.
- [16] G. Y. Gu, J. Zhu, L. M. Zhu, and X. Zhu, "A survey on dielectric elastomer actuators for soft robots," *Bioinspiration and Biomimetics*, vol. 12, no. 1, 2017.
- [17] R. Altmüller, R. Schwödianer, R. Kaltseis, S. Bauer, and I. M. Graz, "Large area expansion of a soft dielectric membrane triggered by a liquid gaseous phase change," *Appl. Phys. A Mater. Sci. Process.*, vol. 105, no. 1, pp. 1–3, 2011.
- [18] H. Yuk, S. Lin, C. Ma, M. Takaffoli, N. X. Fang, and X. Zhao, "Hydraulic hydrogel actuators and robots optically and sonically camouflaged in water," *Nat. Commun.*, vol. 8, pp. 1–12, 2017.
- [19] X. Gong *et al.*, "Rotary Actuators Based on Pneumatically Driven Elastomeric Structures," *Adv. Mater.*, pp. 7533–7538, 2016.
- [20] S. Konishi, S. Shimomura, S. Tajima, and Y. Tabata, "Implementation of soft microfingers for a hMSC aggregate manipulation system," *Microsystems Nanoeng.*, vol. 2, no. March 2015, 2016.
- [21] Y. Sun, Y. S. Song, and J. Paik, "Characterization of silicone rubber based soft pneumatic actuators," *IEEE Int. Conf. Intell. Robot. Syst.*, pp. 4446–4453, 2013.
- [22] J. A. Menéndez *et al.*, "Microwave heating processes involving carbon materials," *Fuel Process. Technol.*, vol. 91, no. 1, pp. 1–8, 2010.



- [23] W. Wang, Y. Liu, and J. Leng, "Recent developments in shape memory polymer nanocomposites: Actuation methods and mechanisms," *Coord. Chem. Rev.*, vol. 320–321, pp. 38–52, 2016.
- [24] H. Kim, K. Kim, and S. J. Lee, "Nature-inspired thermo-responsive multifunctional membrane adaptively hybridized with pnipam and ppy," *NPG Asia Mater.*, vol. 9, no. 10, 2017.
- [25] X. Dong *et al.*, "Sunlight-Driven Continuous Flapping-Wing Motion," *ACS Appl. Mater. Interfaces*, vol. 12, no. 5, pp. 6460–6470, 2020.
- [26] T. J. White *et al.*, "A high frequency photodriven polymer oscillator," *Soft Matter*, vol. 4, no. 9, pp. 1796–1798, 2008.
- [27] H. Yang *et al.*, "Multifunctional metallic backbones for origami robotics with strain sensing and wireless communication capabilities," *Sci. Robot.*, vol. 4, no. 33, pp. 1–14, 2019.
- [28] M. De Volder and D. Reynaerts, "Pneumatic and hydraulic microactuators: A review," *J. Micromechanics Microengineering*, vol. 20, no. 4, 2010.
- [29] T. Xu, J. Zhang, M. Salehizadeh, O. Onaizah, and E. Diller, "Millimeter-scale flexible robots with programmable three-dimensional magnetization and motions," *Sci. Robot.*, vol. 4, no. 29, 2019.
- [30] E. Diller, J. Zhuang, G. Zhan Lum, M. R. Edwards, and M. Sitti, "Continuously distributed magnetization profile for millimeter-scale elastomeric undulatory swimming," *Appl. Phys. Lett.*, vol. 104, no. 17, 2014.
- [31] X. Ji *et al.*, "An autonomous untethered fast soft robotic insect driven by low-voltage dielectric elastomer actuators," *Sci. Robot.*, vol. 4, no. 37, 2019.
- [32] Y. Wu *et al.*, "Insect-scale fast moving and ultrarobust soft robot," *Sci. Robot.*, vol. 4, no. 32, 2019.
- [33] T. Li, K. Nakajima, M. Calisti, C. Laschi, and R. Pfeifer, "Octopus-inspired sensorimotor control of a multi-arm soft robot," *2012 IEEE Int. Conf. Mechatronics Autom. ICMA 2012*, pp. 948–955, 2012.
- [34] S. M. Felton *et al.*, "Self-folding with shape memory composites," *Soft Matter*, vol. 9, no. 32, pp. 7688–7694, 2013.
- [35] J. Liu *et al.*, "Dual-Gel 4D Printing of Bioinspired Tubes," *ACS Appl. Mater. Interfaces*, vol. 11, no. 8, pp. 8492–8498, 2019.
- [36] M. Boyvat, D. M. Vogt, and R. J. Wood, "Ultrastrong and High-Stroke Wireless Soft Actuators through Liquid – Gas Phase Change," vol. 1800381, pp. 1–6, 2018.
- [37] J. Han *et al.*, "Untethered Soft Actuators by Liquid–Vapor Phase Transition: Remote and Programmable Actuation," *Adv. Intell. Syst.*, vol. 1, no. 8, p. 1900109, 2019.
- [38] H. Banerjee, M. Suhail, and H. Ren, "Hydrogel actuators and sensors for biomedical soft robots: Brief overview with impending challenges," *Biomimetics*, vol. 3, no. 3, pp. 1–41, 2018.
- [39] T. Applications, "Microfluidics," pp. 523–548.
- [40] L. Ionov, "Hydrogel-based actuators: Possibilities and limitations," *Mater. Today*, vol. 17, no. 10, pp. 494–503, 2014.
- [41] P. Calvert, "Gel sensors and actuators," *MRS Bull.*, 2008.
- [42] A. Miriyev, K. Stack, and H. Lipson, "Soft material for soft actuators," *Nat. Commun.*, vol. 8, no. 1, pp. 1–8, 2017.
- [43] X. Shen, J. L. Shamshina, P. Berton, G. Gurau, and R. D. Rogers, "Hydrogels based on cellulose and chitin: Fabrication, properties, and applications," *Green Chem.*, vol. 18, no. 1, pp. 53–75, 2015.
- [44] Y. Geng, P. L. Almeida, S. N. Fernandes, C. Cheng, P. Palfy-Muhoray, and M. H. Godinho, "A cellulose liquid crystal motor: A steam engine of the second kind," *Sci. Rep.*, vol. 3, pp. 1–5, 2013.
- [45] M. M. Hamed *et al.*, "Electrically Activated Paper Actuators," *Adv. Funct. Mater.*, vol. 26, no. 15, pp. 2446–2453, 2016.
- [46] J. Kim, S. Yun, S. K. Mahadeva, K. Yun, S. Y. Yang, and M. Maniruzzaman, "Paper

- actuators made with cellulose and hybrid materials,” *Sensors*, vol. 10, no. 3, pp. 1473–1485, 2010.
- [47] H. P. Phan *et al.*, “Self-sensing paper-based actuators employing ferromagnetic nanoparticles and graphite,” *Appl. Phys. Lett.*, vol. 110, no. 14, 2017.
- [48] A. S. Chen, H. Zhu, Y. Li, L. Hu, and S. Bergbreiter, “A paper-based electrostatic zipper actuator for printable robots,” *Proc. - IEEE Int. Conf. Robot. Autom.*, pp. 5038–5043, 2014.
- [49] T. Harvard, “Mechanics of Soft Actuators,” 2018.
- [50] S. Moise, E. Céspedes, D. Soukup, J. M. Byrne, A. J. El Haj, and N. D. Telling, “The cellular magnetic response and biocompatibility of biogenic zinc- and cobalt-doped magnetite nanoparticles,” *Sci. Rep.*, vol. 7, no. January, pp. 1–11, 2017.
- [51] D. Wen, “Nanoparticle-related heat transfer phenomenon and its application in biomedical fields,” *Heat Transf. Eng.*, vol. 34, no. 14, pp. 1171–1179, 2013.
- [52] D. Gao *et al.*, “Photothermal actuated origamis based on graphene oxide-cellulose programmable bilayers,” *Nanoscale Horizons*, vol. 5, no. 4, pp. 730–738, 2020.
- [53] Z. Chen, J. Liu, Y. Chen, X. Zheng, H. Liu, and H. Li, “Multiple-Stimuli-Responsive and Cellulose Conductive Ionic Hydrogel for Smart Wearable Devices and Thermal Actuators,” *ACS Appl. Mater. Interfaces*, vol. 13, no. 1, pp. 1353–1366, 2021.
- [54] G. Wang *et al.*, “Printed paper actuator: A low-cost reversible actuation and sensing method for shape changing interfaces,” *Conf. Hum. Factors Comput. Syst. - Proc.*, vol. 2018-April, pp. 1–12, 2018.
- [55] A. Toncheva *et al.*, “Fast IR-Actuated Shape-Memory Polymers Using in Situ Silver Nanoparticle-Grafted Cellulose Nanocrystals,” *ACS Appl. Mater. Interfaces*, vol. 10, no. 35, pp. 29933–29942, 2018.
- [56] M. Amjadi and M. Sitti, “High-Performance Multiresponsive Paper Actuators,” *ACS Nano*, vol. 10, no. 11, pp. 10202–10210, 2016.
- [57] P. Kulkarni, “Centrifugal Forming and Mechanical Properties of Silicone-Based Elastomers for Soft Robotic Actuators,” no. October 2015, 2015.
- [58] Y. Yu *et al.*, “Multifunctional ‘Hydrogel Skins’ on Diverse Polymers with Arbitrary Shapes,” *Adv. Mater.*, vol. 31, no. 7, pp. 1–9, 2019.
- [59] S. H. Kim, S. Jung, I. S. Yoon, C. Lee, Y. Oh, and J. M. Hong, “Ultrastretchable Conductor Fabricated on Skin-Like Hydrogel–Elastomer Hybrid Substrates for Skin Electronics,” *Adv. Mater.*, vol. 30, no. 26, pp. 1–8, 2018.
- [60] Y. Qian *et al.*, “Octopus tentacles inspired triboelectric nanogenerators for harvesting mechanical energy from highly wetted surface,” *Nano Energy*, vol. 60, no. February, pp. 493–502, 2019.
- [61] Y. Fouillet *et al.*, “Stretchable Material for Microfluidic Applications,” *Proceedings*, vol. 1, no. 10, p. 501, 2017.
- [62] A. Materials, “No Title.” [Online]. Available: <https://www.azom.com/properties.aspx?ArticleID=1461>. [Accessed: 12-Dec-2020].
- [63] M. P. Database, “No Title.” [Online]. Available: <http://www.mit.edu/~6.777/matprops/pmma.htm>.
- [64] DESIGNERDATA, “No Title.” [Online]. Available: <https://designerdata.nl/materials/plastics/rubbers/nitrile-butadiene-rubber>. [Accessed: 12-Dec-2020].

Annex

This annex provides additional information concerning the Results and Discussion section.

Table A.1 - Results of testing different elastomers and double-sided tapes.

	Latex glove (85 μm)	Nitrile glove (69 μm)
Double-sided tape (54 μm)		
Double-sided tape stickier (209 μm)	